LAYER-BY-LAYER ASSEMBLED SMECTITE-POLYMER NANOCOMPOSITE FILM FOR RAPID DETECTION OF LOW-CONCENTRATION AFLATOXINS

A Thesis

by

HE HU

Submitted to the Office of Graduate Studies of
Texas A&M University
in partial fulfillment of the requirements for the degree of

MASTER OF SCIENCE

Approved by:

Chair of Committee,	Jun Zou
Committee Members,	Youjun Deng
	Jim Xiuquan Ji
	Jun Kameoka
Head of Department,	Chanan Singh

December 2012

Major Subject: Electrical Engineering

ABSTRACT

Aflatoxin is a potent biological toxin produced by fungi *Aspergillus flavus* and *A. parasiticus.* Current quantification methods for aflatoxins are mostly established on immunoaffinity columns which are both costly and labor intensive. Inspired by smectites' high aflatoxin adsorption capacity and affinity, a novel aflatoxin quantification sensor based on smectite-polyacrylamide (PAM) nanocomposite was fabricated. First, a smectite-PAM nanocomposite film was synthesized on flat silicon substrates which assembled smectite particles from the clay suspension. A layer-by-layer assembly process was developed to achieve uniform morphology and thickness of the nanocomposite films. During the aflatoxin quantification process, positive correlations between the fluorescence intensity from the aflatoxin B_1 (AFB_1) adsorbed smectite-PAM nanocomposite films and the AFB_1 concentration in the test solutions were obtained. The smectite-PAM nanocomposite film has shown similar AFB_1 adsorption capabilities as the smectite.

Second, the smectite-PAM nanocomposite film was optimized in order to achieve the aflatoxin quantification at ppb level (below 20ppb) in corn extraction solutions. The smectite was modified by Ba^{2+}, which had demonstrated to be able to improve its aflatoxin adsorption capacity. PAM aqueous solutions with the mass concentration ranging from 0.8% to 0.001% were tested. The results showed that the nanocomposite synthesized from 0.005% concentration of PAM solution generated the best properties. After the optimization, the smectite-PAM nanocomposite films achieved

the detection of aflatoxin B_1, B_2, G_1 and G_2 (AFB_2, AFG_1 and AFG_2) in 10 ppb corn extraction solution. Aflatoxin quantifications in AFB_1 and AFB_2 mixture solution, AFB_1 and AFB_2 mixture solution and AFB_1 and AFG_1 mixture solution were conducted, and the recoveries of last test ranged from 90.52% to 110.11% at low aflatoxin concentration (below 20 ppb).

Third, in order to shorten the quantification duration and simplify the detection process, a novel aflatoxin detection array based on smectite-PAM nanocomposite and an improved fluorometric quantification method were developed. Through a microfluidic chip, the reaction time was reduced to 10~20min. Two concentration levels (20~80ppb/5~15ppb) of aflatoxin B_1 spiked corn extraction solutions were tested. In the fluorometric quantification step, a common lab-use 365 nm ultraviolet lamp replaced the spectrofluorometer which simplified and accelerated the process.

To my parents and all those who once encouraged me

ACKNOWLEDGEMENTS

I would like to thank my committee chair, Dr. Jun Zou, and my committee members, Dr. Youjun Deng, Dr. Kameoka Jun, and Dr. Jim Xiuquan Ji, for their guidance and support throughout the course of this research.

Thanks also go to Mr. Robert Atkins and Mr. Jim Gardner my friends for their technical training, support and collaboration throughout my entire research and fabrication steps. I also want to extend my gratitude to my colleagues in this research such as Ms. Ana Barrientos Velazquez and Ms. Lian Liu for helping prepare materials and facilities. And my friends Alejandro, Alex, Young, Chih-Hsien, Ryan, Kenneth To, Jianwei Zhou, Hongfei Liang, Jialong Zhang and Chen Lin for their encouragement and support during the past two memorable years.

Finally, thanks to my mother and father for their love, which is the most endless, selfless and priceless love in the world.

TABLE OF CONTENTS

Page

Page

LIST OF FIGURES

Page

Page

Page

LIST OF TABLES

Page

1. INTRODUCTION

Mycotoxins are toxic metabolite produced by fungi such as *Aspergillus*, *Penicillium*, and *Fusarium*. As estimated by The Food and Agriculture Organization (FAO) of the United Nations, 25% of the world's food crops are affected by mycotoxin producing fungi and nearly one billion tons of food stuff is lost because of mycotoxin contamination every year. Aflatoxins, fumonisins, ocharatoxin A, deoxynivalenol, and zearalenone are the five agriculturally important mycotoxins [1] (Figure 1).

Mycotoxin occurrence is currently unavoidable due to problems such as drought, heat, insect, humidity, or other stresses. Severe health problems like growth retardation, liver cancer, immunosuppression, endocrine disruption, childhood stunting, neural tube defects and mutagenicity can be caused by the accumulation of mycotoxins in human foods and animal feeds.

Aflatoxins (especially aflatoxin B_1, AFB_1), as a major type of biological toxins, are harmful by-products of the fungi (*Aspergillus flavus* and *A. parasiticus*). As they can cause acutely toxic and carcinogenic effects on human and animal health [2], their contaminations in agricultural commodities, human food and animal feed have become major concerns in the food and feed industries. Therefore, rapid, quantitative and low-cost detection methods are critical for the timely evaluation, monitoring and mitigation of the hazardous effects caused by aflatoxins. Currently, the "gold standard" for aflatoxins detection is the high-performance liquid chromatography (HPLC) followed by fluorometric or mass spectroscopic analysis [2,3], which is time-consuming and costly,

and thus it is mainly limited to laboratory uses. In the past few years, a number of rapid detection methods based on immunoassays have been developed [4,5]. These methods utilize antibodies to selectively capture aflatoxins from the test solution [6-8]. In spite of their high adsorption selectivity and affinity, the antibodies are susceptible to denaturation and degradation, and therefore stringent testing conditions are necessary to ensure their performance. In addition, the production of antibodies requires live animals, which is a complex and expensive process.

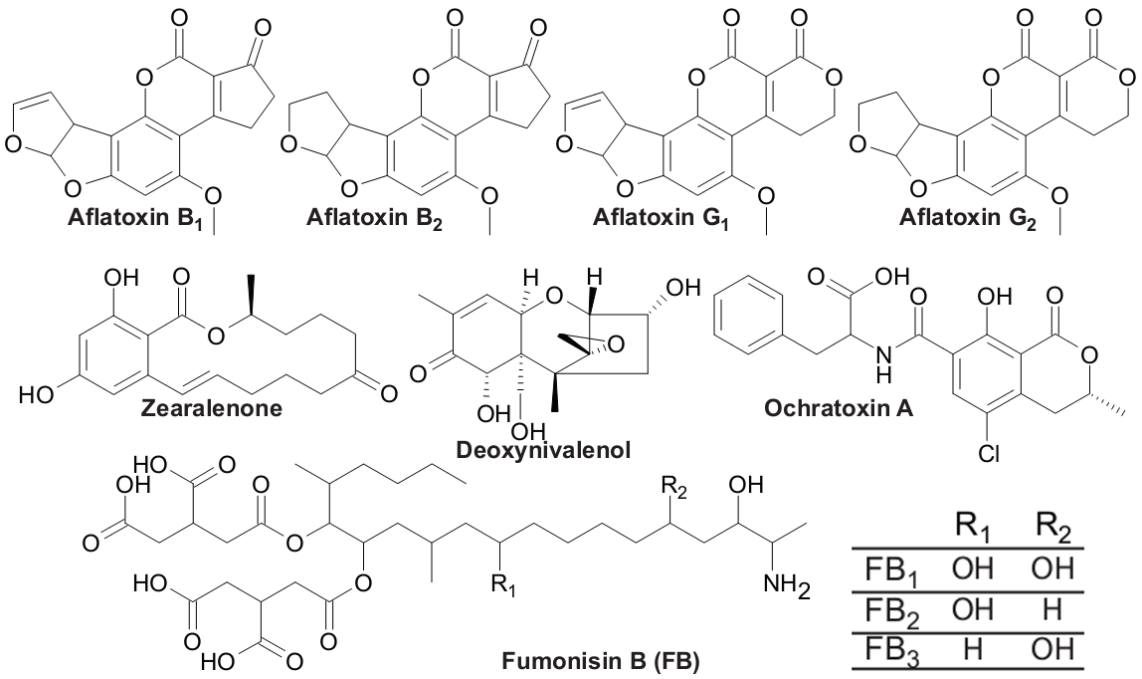

Figure 1. Five major mycotoxins: aflatoxins, fumonisins, ochratoxin A, deoxynivlalenol, and zearalenone [1].

To further reduce the cost, to increase the supplies, and to make the quantification more robust, many researchers are exploring alternative molecular recognition compounds for mycotoxin quantification. Natural and modified clay minerals, for example smectites, have shown high adsorption capacity and selectivity for mycotoxins. During the last three decades, several bentonites (smectite-rich clays) have been used as adsorbent additives to detoxify aflatoxin-contaminated animal feeds [9]. Recent studies have shown that the divalent cations and transition cations in the interlayers of smectite can induce the substantial binding of AFB_1 to the smectite [10]. Unlike the antibodies, the smectite-AFB_1 binding is not drastically affected by adsorption conditions, e.g., temperature or pH value. In addition, a high adsorption capacity (e.g., 10~20% of the self weight of the smectite [11]) can also be obtained due to the large surface area (about 800 m^2/g) of the smectite. Because of its high adsorption selectivity and capacity for AFB_1, it is possible to use smectite as an inexpensive inorganic molecular recognition agent to replace the delicate and costly antibodies for mycotoxin quantification. However, due to its small particle size and tendency to disperse in water or solvents, it is difficult to directly use smectite as the biosensor for mycotoxin detection.

On the other side, array biosensing is one of the emerging techniques in rapid mycotoxin quantification. It has been successfully used to quantify the major types of mycotoxins. Yet, it has been realized that many antibodies cannot differentiate the subtle differences in one group of mycotoxins such as aflatoxin B_1, B_2, G_1 and G_2 (Figure 1), which differ only in one bond, one atom, or one functional group. Quantification of these

individual toxins still needs further chromatographic separation with sophisticated HPLC methods. It is desirable if the molecular recognition agents can both concentrate a group of mycotoxins and can chromatographically separate the individual mycotoxins within the same group that have closely-resembled molecular structures.

Based on the advances achieved in the past two decades on interactions of clay minerals with various small organic compounds and polymers, in this study, a kind of smectite-polymer nanocomposite film was first synthesized for aflatoxin quantification in food extraction solutions. In addition, the optimization of this nanocomposite material was investigated and demonstrated to be able to improve its aflatoxin adsorption capacity. Finally, a simple but effective microfluidic sensor for aflatoxin quatification based on smectite-polymer nanocomposite film was developed and tested in real food extraction solution.

In section 2, the synthesis process of the smectite-polymer nanocomposite film was introduced. A layer-by-layer assembly method was taken to bound polymer chain molecules with smectite micro-particles in the clay suspension. After that, results of initial aflatoxin quantification tests through the nanocomposite film were analyzed in detail.

In section 3, the optimization process of the nanocomposite film was described. And the following aflatoxin quantification tests proved the optimized nanocomposite film could quantify aflatoxins at ppb level. In addition, its adsorption capacities on different types of aflatoxins were investigated. A fluorometric method on quantifying different types of aflatoxins in food extraction solutions was developed and verified.

In section 4, a microfluidic aflatoxin quantification chip based on smectite-polymer nanocomposite film was introduced. Through using this microfluidic chip, the aflatoxin quantification duration was reduced to 10~20 min. In addition, the high precision spectrofluorometer in the quantification process was replaced by a low cost lab use ultraviolet lamp, which reduced the total cost and complexity of the quantification process.

2. LAYER-BY-LAYER ASSEMBLED SMECTITE-POLYMER NANOCOMPOSITE FILM FOR RAPID FLUOROMETRIC DETECTION OF AFLATOXIN B_1*

2.1 INTRODUCTION

Smectite particles are usually several micrometers in dimension, and they tend to disperse in water or solvents, which makes it difficult to directly use them in biosensors for aflatoxin detection. In this section, a layer-by-layer assembly approach to synthesize smectite-polyacrylamide (PAM) nanocomposite films on flat silicon substrates was introduced. And the application of these films to the quantification of AFB_1 in aqueous and corn extraction solutions was also presented. The layer-by-layer assembly method provided good morphology and thickness control of the nanocomposite film. In the aflatoxin quantification tests, different from previous fluorometric characterization methods (by measuring the fluorescence intensity of the eluent solutions [12-14]), the fluorescence emission spectra of AFB_1 adsorbed nanocomposite films were characterized. Strong correlations between the peak fluorescence intensity of the AFB_1 adsorbed to the nanocomposite film and the AFB_1 concentration in the test solution were identified. Based on the test results, the smectite-PAM nanocomposite film proved to be able to work as an effective sensing material in the direct fluorometric quantification of the AFB_1 (without the elution steps).

---

*Reprinted from Sensor and Actuator B: Chemical, Vol. 166-167, He Hu, Alejandro Garcia-Uribe, Youjun Deng and Jun Zou, Layer-by-layer assembled smectite-polymer nanocomposite film for rapid fluorometric detection of aflatoxin B_1, Page No. 205-211, Copyright (2012), with permission from Elsevier.

2.2 MATERIALS AND METHODS

2.2.1 Smectite preparation

Unless otherwise noted, the following preparation procedures were performed at the room temperature. A Greek calcium bentonite was obtained from the S&B Industrial Minerals S.A. (1934-now, Athens, Greece). Our X-ray diffraction (XRD) and infrared spectroscopy analysis (data not shown) indicated that its mineral composition was dominated by the smectite containing a small amount of calcite, quartz and feldspars. To extract relative pure smectite, 10 g of the bentonite was dispersed in a diluted (pH 10) Na_2CO_3 solution, and then the < 2 μm clay fraction was separated by the sedimentation method. The collected clay particles were stored in a suspension solution.

2.2.2 Layer-by-layer assembly smectite-PAM nanocomposite films

The smectite-PAM nanocomposite film was synthesized on flat silicon substrates through a layer-by-layer assembling process. Since the smectite was negatively charged, a positively charged copolymer (PAM 494C obtained from Kemira Chemicals, Inc, Atlanta, GA) was used in the layer-by-layer assembly. This copolymer contained 80% nonionic acrylamide units and 20% cationic N,N,N-trimethyl-aminoethyl acrylate units [15]. The multiple points of electrostatic attractions between the cationic functional groups of PAM chains and the negative charge sites of the smectite, combining with the high entropy gain from water replacement by the polymer, made the smetite-polymer complexes stable in both water and solvents [16]. The random arrangement of the smectite in the nanocomposite matrix also helped to increase its porosity and binding site accessibility for AFB_1 molecules [17].

A single-crystalline silicon wafer (4" P (100) 0-100 ohm-cm SSP 500um Test wafers), purchased from University Wafer, Inc. (South Boston, MA), was used as the substrate for the layer-by-layer assembly of the smectite-PAM nanocomposite film. Single-crystalline silicon did not manifest optical fluorescence that would interfere with that from AFB_1 molecules. The pristine surface condition and high reflectivity of the single-crystalline silicon wafers also helped the assembly, characterization and testing of the smectite-PAM nanocomposite film. The silicon wafer was diced into rectangular pieces (13×15 mm^2), such that they could be snuggly fit into the sample holder of a spectrofluorometer used in this study. It should be noted that the layer-by-layer assembly process is substrate-independent and can be performed on other substrates as well.

The layer-by-layer assembly was conducted using 1 g/L PAM aqueous solution and 1 g/L smectite aqueous dispersion as described below [18]: 1) a group of pre-cleaned silicon substrates were immersed into the PAM solution for 7 min and then rinsed in deionized (DI) water for 2 min to remove excessive PAM coating on the surface; 2) the silicon substrates were immersed in the smectite dispersion for 5 min and rinsed in DI water for 2 min; and 3) the above cycle was repeated ~30 times until the silicon substrate surface was fully covered with the nanocomposite film. The immersion times in steps 1) and 2) were determined based on a preliminary trial of the growth rate and quality of nine films after 5, 7, 9 min of immersion in the polymer and clay suspension.

2.2.3 Preparation of AFB_1 aqueous solution

Fifty mg AFB_1 from *Aspergillus Flavus* (Sigma-Aldrich Inc. St. Luis, MO) was dissolved in 50 mL acetonitrile to obtain a 1000 ppm stock solution. An 8 ppm AFB_1 test solution was made by diluting the stocking solution with DI water. AFB_1 aqueous solutions at lower concentrations were prepared by further diluting the 8 ppm solution with DI water.

2.2.4 Smectite-PAM film characterization and AFB_1 quantification

The surface and the cross-section of the assembled smectite-PAM nanocomposite film were inspected under an FEI Quanta® 600 scanning electron microscope. The fluorescence emission spectra of AFB_1 adsorbed smectite suspension and smectite-PAM nanocomposite films were characterized using a PTI QuantaMaster® series spectrofluorometer with an ultraviolet (UV) excitation wavelength of 365 nm.

2.2.4.1 Fluorescence intensity characterization of AFB_1 spiked smectite suspension.

A series of 1 mL of 1 g/L smectite suspensions were mixed with different amounts of 8 ppm AFB_1 solutions to achieve AFB_1 mass loadings of 0, 0.25%, 0.5%, 1.0% and 1.5% of the smectite, respectively. Since the maximal AFB_1 mass loading concentration (1.5%) was much lower than the typical absorption capacity (10~20%) of the smectite [10], we believe most of AFB_1 molecules would adsorb into the smectite. After letting the mixture react overnight, each of the mixed suspensions was injected into an ink-well device made of a poly(methyl methacrylate) (PMMA) substrate bonded with a micro-molded polydimethylsiloxane (PDMS) structure. Water was evaporated at 70 ^{o}C. In the ink-wells, the spread area of the mixture during the drying process was

well-controlled. A uniform thickness of the resulting smectite film was obtained to ensure a consistent measurement of the fluorescence intensity. The reasons for using ink-wells are that the spectrofluorometer only samples and integrates the fluorescence signal from a certain area (about 5×5 mm^2) of the surface of the sample and the fluorescence intensity is affected by both the AFB_1 concentration and the film thickness of the sampled region.

2.2.4.2 Fluorescence intensity characterization of AFB_1 adsorbed smectite-PAM nanocomposite films.

A total of 32 smectite-PAM nanocomposite films on silicon substrates were prepared, and tested in one control (DI water, 2 mL) and seven AFB_1 aqueous solutions (0.2, 0.4, 0.8, 1.0, 2.0, 4.0 and 8.0 ppm, 2 mL for each), with four replications for each concentration. To determine an optimal immersion time for AFB_1 adsorption, six smectite-PAM nanocomposite films were prepared and five of them were immersed into AFB_1 aqueous solutions (4.0 ppm, 2 mL for each) for 10, 30, 40, 60 and 90 min, respectively. The 4.0 ppm AFB_1 aqueous solution was chosen to provide good fluorescence signal strength (with a high signal-to-noise ratio) without saturating the AFB_1 adsorption of the smectite-PAM nanocomposite film. The fluorescence spectra of the AFB_1 adsorbed nanocomposite films were recorded. The fluorescence spectra of AFB_1 solutions before and after the adsorption were also recorded to calculate the AFB_1 concentrations of the solutions.

2.2.5 AFB_1 quantification in corn extraction solution

To demonstrate the feasibility of the smectite-PAM nanocomposite film for AFB_1 quantification in agricultural products, a group of these nanocomposite films were immersed into corn extraction solutions spiked with known amounts of AFB_1 and the fluorescence spectra of these films after the immersion were recorded. The corn extraction solution was collected by following the standard aflatoxin extraction and analysis procedures outlined in reference [19]: 1) 50g of corn flour (purchased from a local grocery store) was mixed with 250 mL of extraction solvent (volume ratio of methanol to water is 70:30) in a 500 mL Erlenmeyer flask and the mixture was shaken for 1 hour on a rotary shaker at 200 rpm; 2) the mixture was filtered through a medium-fast filter paper; 3) the extract was split into a series of 50 mL plastic centrifuge tubes within each tube a 10 mL of extract was transferred; 4) A small scoop of sodium chloride (for flocculation) and 20 mL DI water were added into each tube; and 5) all the samples were shaken and filtered through a microfiber filter to remove the oil droplets and flocculated particles. The filtered extract was collected into clean plastic centrifuge tube. Different amounts of AFB_1 were added to the extracts to achieve AFB_1 concentrations of 0, 0.2, 0.4, 0.8, 1.0, 2.0, and 4.0 ppm, respectively. A total of 28 smectite-PAM nanocomposite films were prepared, and then separately immersed into these AFB_1 spiked extracts (2 mL for each) and one control extract (no AFB_1, 2 mL) for 50 min, with four replications for each concentration. The fluorescence spectra of AFB_1 adsorbed smectite-PAM nanocomposite films were recorded as previous films.

2.3 RESULTS AND DISCUSSION

2.3.1 Assembly and characterization of the smectite-PAM nanocomposite film

Uniform and stable smectite-PAM nanocomposite films on silicon wafers were obtained using the layer-by-layer assembly method described in the Material and Method section. Distinct visual differences were observed between the coated (Figure 2, left) and the uncoated (Figure 2, right) wafers. The scanning electron micrographs of the surface (Figure 3A and 3B) and cross-section (Figure 3C and 3D) of the assembled smectite-PAM nanocomposite film (Figure 2, left) show that the micron-scale smectite plates distributed in the PAM matrix with various orientations, which formed a rough and porous film structure. The smectite particles had a similar size and shape with those not mixed with PAM [20]. Therefore, the layer-by-layer assembly process did not significantly change the morphology of the smectite. As shown in Figure 3C and 3D, the nanocomposite film had an intimate contact with the silicon substrate with an overall thickness of 1 ~ 2 μm. Due to the strong electrostatic bonding between the smectite and the PAM molecular chain, the smectite-PAM nanocomposite film was found to remain intact even after being soaked in water for 15 hours.

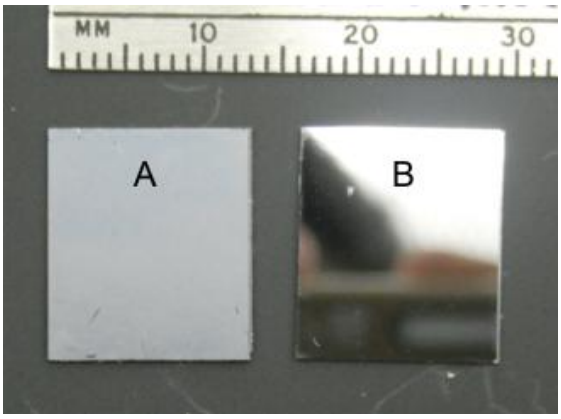

Figure 2. Two single-crystalline silicon substrates: (A) Coated with the smectite-PAM nanocomposite film; (B) Uncoated.

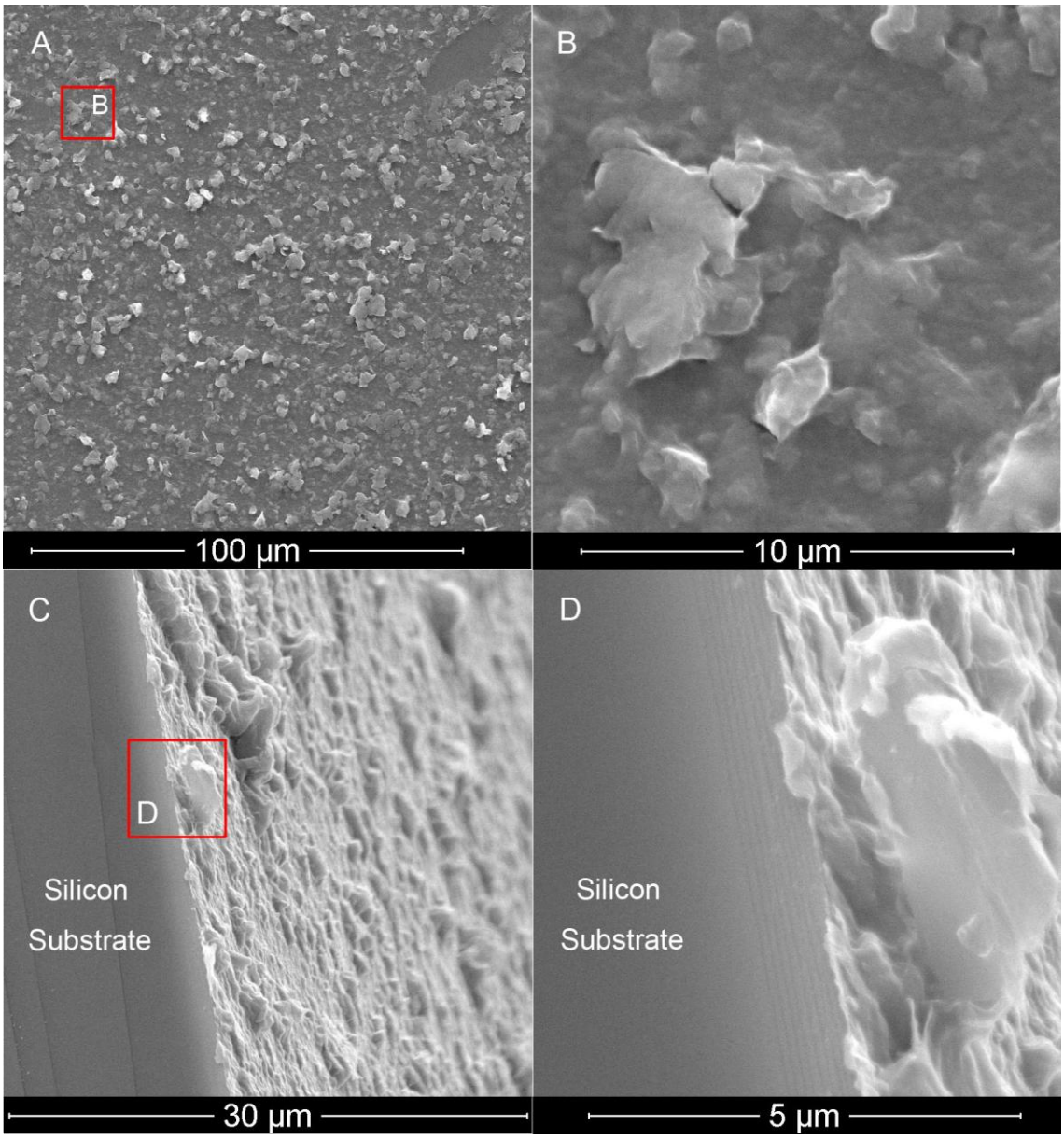

Figure 3. Top (A and B) and side (C and D) views of the smectite-PAM nanocomposite film under a scanning electron microscope.

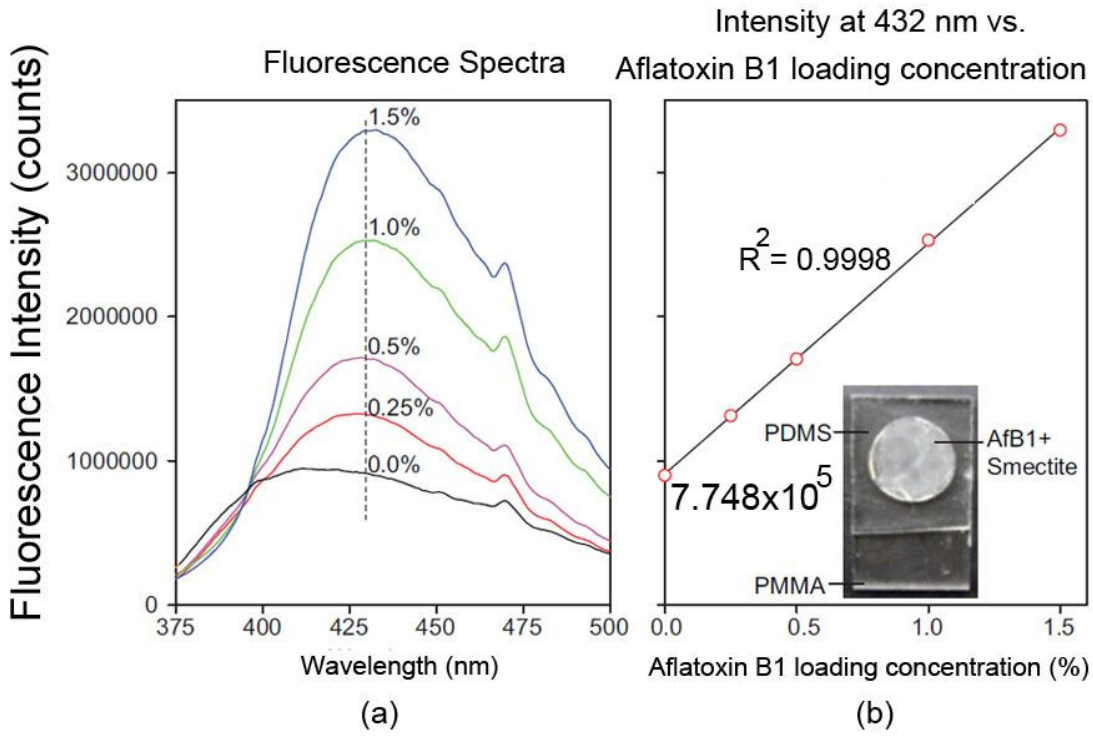

Figure 4. (a) Fluorescence emission spectra of the AFB_1 adsorbed smectite films at different AFB_1 loading concentrations; (b) Peak fluorescence intensity (at 432nm) vs. AFB_1 loading concentration.

2.3.2 Linear correlation between fluorescence intensity and AFB_1 mass loading in AFB_1-smectite mixture

Figure 4a shows the calibrated fluorescence spectra from the four AFB_1-smectite mixtures and a control sample (no AFB_1) after subtracting the background signal (i.e., that from a bare ink-well device). The fluorescence intensities of the four AFB_1-smectite mixtures reached their maximum values around 432 nm. An excellent linear relationship (R^2 = 0.9998) between the peak fluorescent intensity and the mass loading of AFB_1 in the smectite was observed (Figure 4b). This linear correlation indicates the feasibility of

quantifying AFB_1 adsorption onto the smectite by characterizing the peak fluorescence intensity.

2.3.3 Optimal adsorption time of AFB_1 on the smectite-PAM nanocomposite film

Figure 5a shows the calibrated fluorescence spectra from the five immersed smectite-PAM nanocomposite films after subtracting the background signal which was from the films immersed in the DI water. Figure 5b shows the correlation between the peak fluorescence intensity (at 432 nm) and the immersion time. The fluorescence intensity first increased with the immersion time and then reached a plateau after about 50 min, indicating an adsorption/desorption equilibrium state was reached and a longer immersion time would not significantly increase the adsorption or the peak fluorescence intensity. Thus, 50 min was determined as an optimal adsorption time and was used in the following-up adsorption experiments.

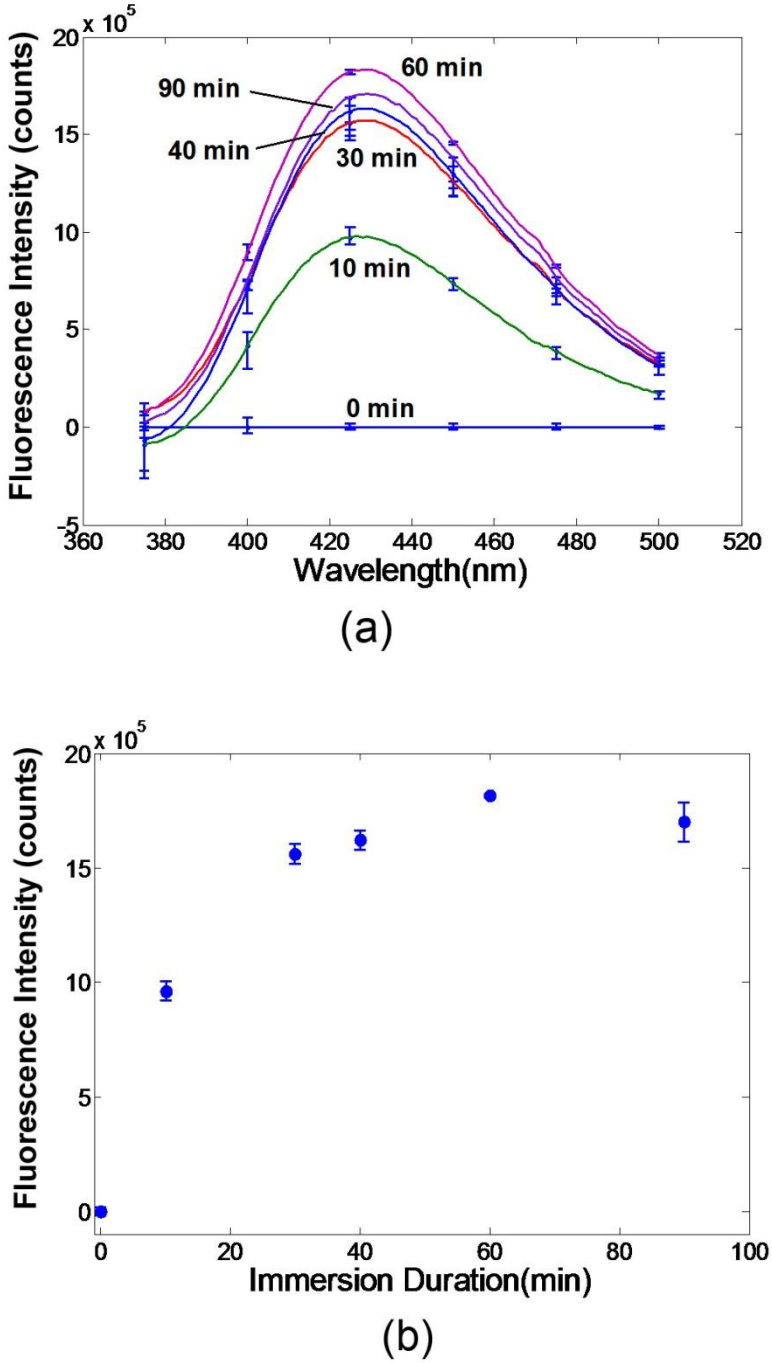

Figure 5. (a) Fluorescence emission spectra and (b) peak fluorescence intensity (at 432nm) of the AFB_1 adsorbed smectite-PAM nanocomposite films after different immersion times.

2.3.4 Correlation between fluorescence intensity and the amount of AFB_1 adsorbed onto the smectite-PAM nanocomposite film

Figure 6a and 6b show the peak fluorescence intensity of the adsorbed AFB_1 (on the smectite-PAM nanocomposite film) as a function of the AFB_1 concentration in the test solution. The peak fluorescence intensity first increased linearly with the AFB_1 concentration and started to saturate at higher AFB_1 concentrations (e.g., > 1 ppm). To explain this phenomenon, the peak fluorescence intensity vs. the mass of the adsorbed AFB_1 was plotted in Figure 6c. The mass of the adsorbed AFB_1 was estimated by comparing the amount of AFB_1 in the test solution before and after the adsorption process. As shown in Figure 6c, the peak fluorescence intensity increased linearly with the mass of the adsorbed AFB_1 ($R^2 = 0.9791$). This result indicates that the saturation in the peak fluorescence intensity was due to the saturation in the AFB_1 adsorption at higher concentrations [21]. Based on the fluorescence intensity values (at 432nm) from 20 blank samples immersed in DI water, the limit of detection (LOD) was 9.72 ppb (estimated by average blank value plus 2 times standard deviation of the blank) and the limit of quantification (LOQ) was 48.60 ppb (estimated by average blank value plus 10 times standard deviation of the blank) [22]. Therefore, under the testing conditions used in our experiments, the linear range of the fluorometric quantification of AFB_1 was from 50 ppb to 1 ppm. However, since the peak fluorescence intensity was proportional to the mass adsorption of AFB_1, lower detection limits comparable to those of the immunoassays (e.g., 1.5~5.1 ppb, [4]) could be readily achieved by increasing the volume of the test solution.

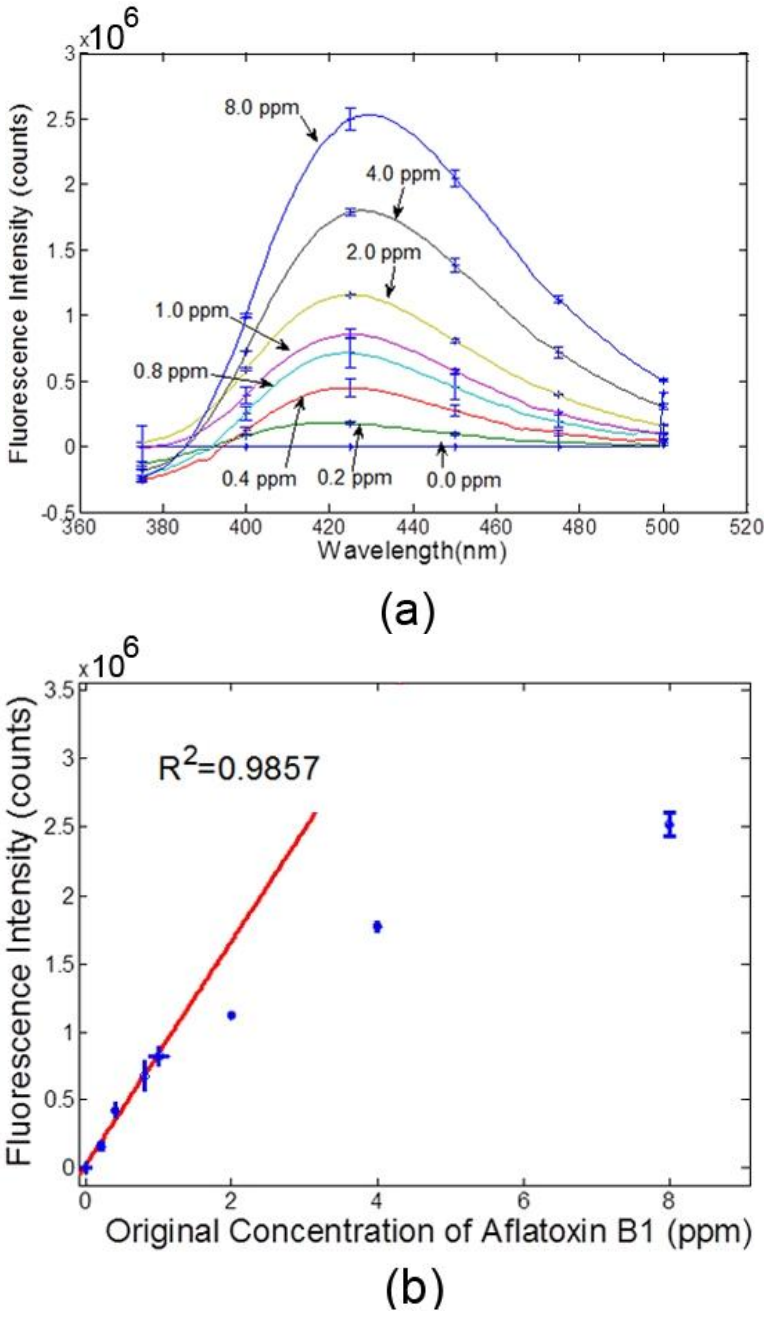

Figure 6. (a) Fluorescence emission spectra of the smectite-PAM nanocomposite films after being immersed in AFB_1 solutions at different concentrations; (b) Peak fluorescence intensity (at 432nm) from the AFB_1 adsorbed nanocomposite films vs. the original AFB_1 concentration in the solution; and (c) Peak fluorescence intensity (at 432 nm) from the AFB_1 adsorbed nanocomposite films vs. the mass of the adsorbed AFB_1.

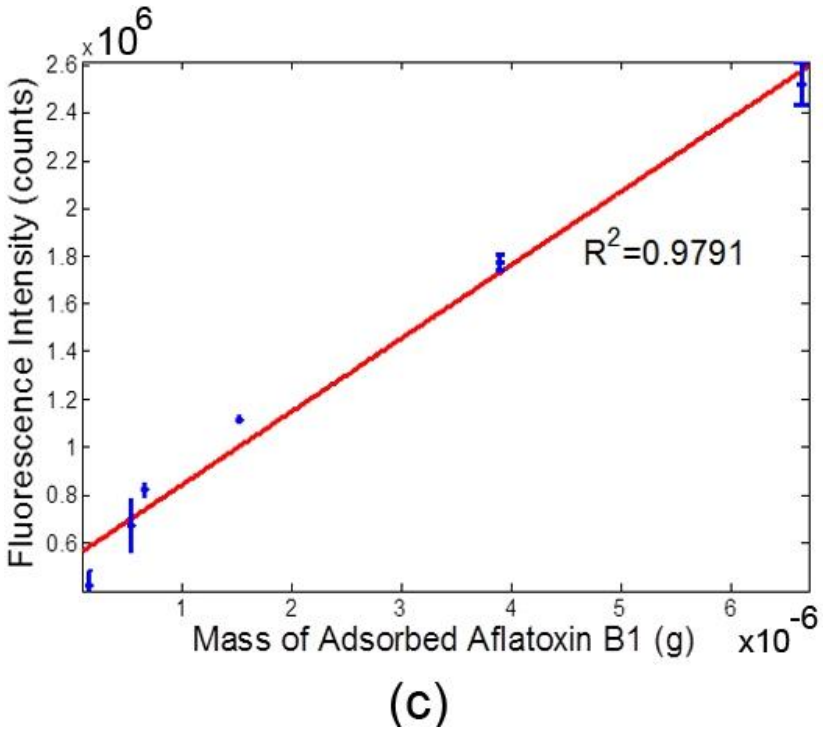

Figure 6. Continued.

2.3.5 Fluorescence intensity of AFB_1 adsorbed smectite-PAM nanocomposite films immersed in corn extraction solutions

Figure 7a shows the fluorescence emission under a UV lamp and Figure 7b shows the spectra under the 365nm UV excitation from one group of semectite-PAM nanocomposite films immersed in AFB_1 spiked corn extraction solutions without agitation. The smectite-PAM nanocomposite films had a similar adsorption property as that in the pure aqueous solutions (see Figure 7b) but with the lower peak fluorescence intensity, which indicated that fewer AFB_1 molecules adsorbed to the smectite-PAM nanocomposite film. To investigate the possibility of any competing adsorption from

other contents in the corn extract solution, the adsorption experiment was repeated with agitation by an orbital shaker at 80 rpm and the resulting fluorescence and spectra are shown in Figure 7c and 7d, respectively. As indicated by the average and standard deviation of the peak fluorescence intensity (at 432 nm) from these two groups of nanocomposite films (with/without agitation) (Figure 7e), the peak fluorescence intensity, and thus AFB_1 adsorption, increased by two to three times through agitation. The fluorescence intensity was even higher than that obtained from the AFB_1 aqueous solutions. Based on the above results, it can be concluded that if there is any, the competing adsorption from other contents in the corn extract solution should not significantly interfere with the AFB_1 adsorption. Compared with aqueous solutions, corn extraction solutions are more viscous and thus more difficult for AFB_1 molecules to diffuse. Therefore, applying agitation can increase their diffusion and adsorption onto the smectite-PAM nanocomposite film.

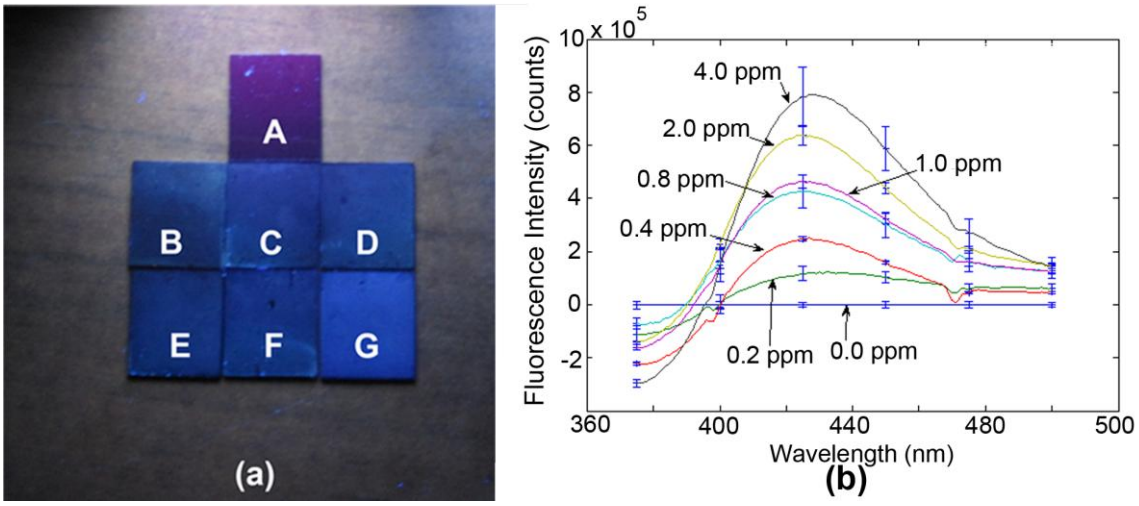

Figure 7. (a) and (c) Photos of the smectite-PAM nanocomposite films under 365nm UV light after being immersed in AFB_1 spiked corn extraction solutions (without/with agitation): (A) 0.0ppm, (B) 0.2ppm, (C) 0.4ppm, (D) 0.8ppm, (E) 1.0ppm, (F) 2.0ppm and (G) 4.0ppm; (b) and (d) Fluorescence emission spectra of the smectite-PAM nanocomposite films after being immersed in AFB_1 spiked corn extraction solutions at different concentrations (without/with agitation); (e) Peak fluorescence intensity (at 432nm) from the AFB_1 adsorbed nanocomposite films (with/without agitation) vs. the original AFB_1 concentration in the corn extraction solution.

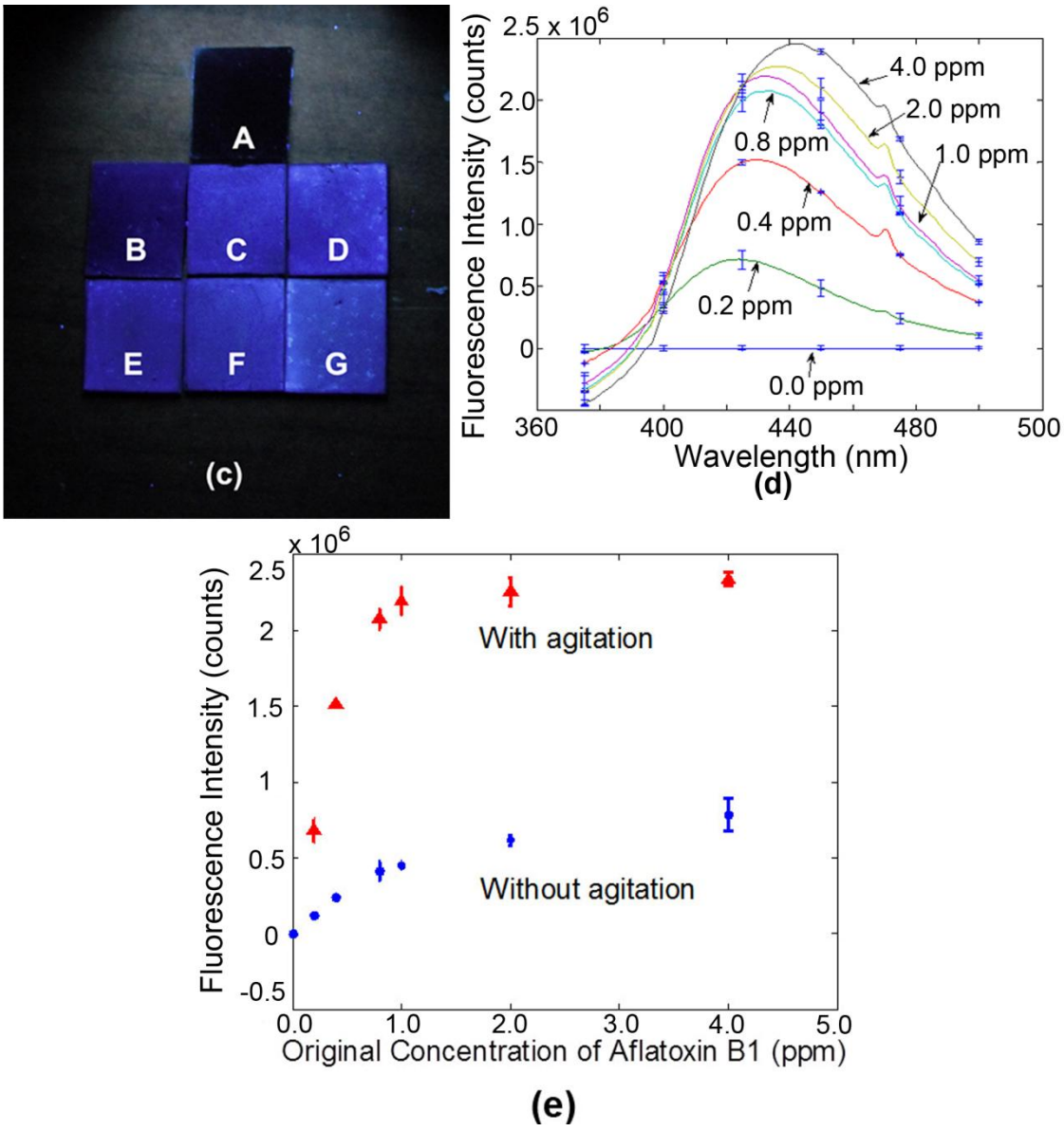

Figure 7. Continued.

2.4 CONCLUSION

In conclusion, the layer-by-layer assembly of smectite-PAM nanocomposite film and the fluorescence characterization of the adsorbed AFB_1 on the assembled nanocomposite film were successfully conducted. The layer-by-layer assembly method provided good control of the morphology and thickness of the nanocomposite film, which could be translated onto various substrates for mass production. The experimental results have shown that the smectite-PAM nanocomposite film can maintain similar adsorption properties as the original smectite, while providing excellent structural stability necessary for device fabrication. They also indicate the feasibility to use the smectite-polymer nanocomposite film for direct fluorometric quantification of AFB_1 (without the elution step). This work provides a good foundation for the development of new smectite-PAM nanocomposite based biosensors for the rapid detection of AFB_1. However, the aflatoxin concentration in the solutions tested in this study was still at ppm level which was much higher than the stringent limitations (several ppb) on aflatoxin concentration in the food. Therefore, the research in the next section will focus on the optimization of the smectite-PAM nanocomposite film to maximize its structural stability and capacity for aflatoxin adsorption. Besides it, the adsorption capacities of the smectite-PAM nanocomposite film on different types of aflatoxins should also be investigated.

3. OPTIMIZED SMECTITE-POLYMER NANOCOMPOSITE FILMS FOR RAPID PPB-LEVEL QUANTIFICATION OF AFLATOXINS*

3.1 INTRODUCTION

As a major type of biological toxins, aflatoxins can cause a wide range of contamination among human food and animal feed even at a very low concentration [23]. Many countries have set stringent standards for the aflatoxin concentration in the foods and feeds. For example, the European regulatory maximum level for aflatoxin M_1 (AFM_1) in liquid and powder milk is 0.05ppb [24]. And according to a recent report [25], about 0.3-6.2% of AFB_1 in animal feed is transformed to AFM_1 in milk. Therefore, detecting and quantifying low concentrations of aflatoxins at ppb level are necessary in the food and feed industry. In the last section, smectite-polymer nanocomposite films were synthesized through a layer-by-layer assembly method, which had shown good structural stability in both water and corn extraction solution. With these nanocomposite films, fluorometric experiments were conducted to quantify aflatoxin B_1 in corn extraction solutions. Aflatoxin B_1 concentrations greater than 200 ppb was successfully quantified. But the detection of lower concentration (e.g., < 20 ppb) was not very effective due to inconsistent readings of the weak fluorescence signals.

* Reprinted from Chemical Sensors, Vol. 2, He Hu, Youjun Deng and Jun Zou, Optimized smectite-polymer nanocomposite films for rapid ppb-level quantification of aflatoxins, 6 pages, Copyright (2012), with permission from Simplex Academic Publishers (www.simplex-academic-publishers.com).

In this section, the optimization of the smectite-polymer nanocomposite films was presented. By increasing the affinity of the nanocomposite film for aflatoxins through cation exchanging and lowering the polymer loading in the nanocomposites, sub-100 ppb quantification of aflatoxins was achieved. The cations (e.g., Ca^{2+}) in the original smectite were replaced by a larger radius and lower hydration energy divalent Ba^{2+}. This process could enhance the size matching between the interlayer adsorbing sites and aflatoxin molecules and thereby enhance the selectivity and affinity for aflatoxin adsorption [10]. In addition, different smectite-polymer ratios for the nanocomposite assembly were investigated to reduce the adsorbing sites occupied by the polymers, enhance workability of assembly, and maintain the stability of the nanocomposites. Using the optimized smectite-polymer nanocomposite films, quantitative fluorometric detections of different types of aflatoxins (AFB_1, AFB_2, AFG_1 and AFG_2) and their mixtures at low concentrations (e.g., < 10 ppb) have been successfully achieved.

3.2 EXPERIMENTAL DETAILS

3.2.1 Chemicals and materials

The < 2 μm smectite suspension was prepared based on the Greek calcium bentonite following the clay suspension preparation procedures listed in the previous section. The smectite in the suspension was saturated by Ca^{2+} at the beginning. To exchange the Ca^{2+} ions with Ba^{2+}, twenty mL of the clay suspension was mixed with 20 mL of 0.1 M $BaCl_2$ solution, and the mixture was centrifuged for 15 minutes. After that, the top clear portion of the mixture was removed. The above modification procedure was

repeated to complete the cation exchange in the smectite. The excess electrolyte in the sample was removed by water washing.

AFB_1, AFB_2, AFG_1 and AFG_2 produced by *Aspergillus Flavus* were obtained from Sigma-Aldrich Inc. (St. Louis, MO). The aflatoxins were dissolved separately in acetonitrile to obtain 1000 ppm stock solutions. An 8 ppm working solution for each aflatoxin was made by diluting the stock solution with DI water.

The corn extraction solution was prepared by the standard aflatoxin extraction and analysis procedures described in the previous section.

3.2.2 Apparatus and equipment

The XRD patterns of the smectite-PAM nanocomposite film were recorded on a D8 Bruker Advance X-ray diffractometer. The surface of this nanocomposite film was inspected under an FEI Quanta® 600 scanning electron microscope. The fluorescence emission spectra of aflatoxin adsorbed smectite-PAM nanocomposite films were characterized under a PTI QuantaMaster® series spectrofluorometer with an ultraviolet (UV) excitation wavelength of 365 nm.

3.2.3 Fabrication of smectite-PAM nanocomposite films

The layer-by-layer assembly process was conducted using PAM aqueous solution and smectite aqueous dispersions of different mass concentrations. Procedures were same to the smectite-PAM nanocomposite fabrication procedures described in the last section.

3.2.4 Quantification of single type of aflatoxin in corn extraction solution

For each type of aflatoxins (AFB_1, AFB_2, AFG_1 and AFG_2), different amounts of 8 ppm working solutions were added into the corn extracts to obtain solutions with concentrations of 0, 10, 20, 40, 80 and 100 ppb, respectively. For each concentration, four test solutions (20 mL each) were prepared. In addition, four control solutions (20 mL corn extracts without aflatoxins) were also prepared as the reference [19]. A total of 96 smectite-PAM nanocomposite films were prepared and separately immersed into these test solutions. All the samples were agitated on an orbital shaker at 80 rpm for 50 minutes. The fluorescence spectra of the aflatoxin-adsorbed smectite-PAM nanocomposite films were recorded using the spectrofluorometer.

3.2.5 Quantification of aflatoxin mixtures in corn extraction solution

For the test on solutions containing different types of aflatoxins, corn extraction solutions spiked with both AFB_1 and AFB_2 were prepared. The ratio of the two types of aflatoxins was determined through controlling the volume of the spiked aflatoxin solutions. Each combination included four replicates. The concentrations of AFB_1 and AFB_2 (1:1 ratio) in these solutions ranged from 5 ppb to 25 ppb. Smectite-PAM films were prepared and tested in these solutions following the above steps. Fluorescence spectra of these aflatoxin adsorbed films were recorded. Following the same procedures, the test on the AFG_1 and AFG_2 mixture solutions was conducted.

Two groups of corn extraction solutions spiked with both AFB_1 and AFG_1 were prepared. Each combination included four replicates. In the first group, the concentrations of aflatoxins were: 1) AFB_1 10 ppb, AFG_1 30 ppb; 2) AFB_1 30 ppb,

AFG_1 10 ppb. In the second group, the concentrations of aflatxoins were: 1) AFB_1 10 ppb, AFG_1 10 ppb; 2) AFB_1 20 ppb, AFG_1 20 ppb. Smectite-PAM films were prepared and tested in these solutions following the above steps. Fluorescence spectra of these aflatoxin adsorbed films were recorded under the spectrofluorometer. The fluorescence intensities at 432 nm and 452 nm were measured. Based on the concentration of aflatoxins and their fluorescence intensity from the first group, a quantitative analysis method was developed. Data from the samples in the second group were used to verify the accuracy of this method.

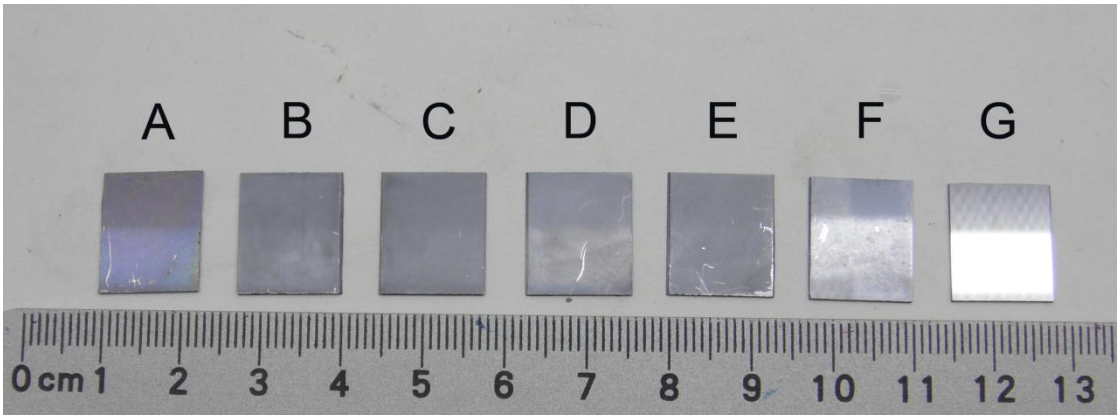

Figure 8. Silicon substrates with smectite-PAM nanocomposite films assembled from PAM solutions with different concentrations:(A) 0.8%, (B) 0.1%, (C) 0.05%,(D) 0.01%,(E) 0.005%,(F) 0.001%,and(G) a bare substrate.

3.3 RESULTS AND DISCUSSION

3.3.1 Assembly and characterization of smectite-PAM nanocomposite films

Six substrates with the smectite-PAM nanocomposite films assembled from (A) 0.8%, (B) 0.1%, (C) 0.05%, (D) 0.01%, (E) 0.005% and (F) 0.001% PAM solutions together with (G) one bare silicon substrate were photographed (Figure 8). The XRD pattern (Figure 9) of the smectite-PAM nanocomposite film assembled from 0.8% PAM solution showed two (001) diffraction peaks at 21.2 Å and 14.3 Å, resepctively. The 21.2 Å diffraction peak was occupation of multiple layers of PAM in the interlayer of smecttie, whereas the 14.3 Å peak was due to only layer or less PAM occupation in the interlayer. As the concentration of the PAM solutions decreased from 0.8% to 0.001%, the diffraction peak representing the multiple layers of PAM occupation diminished, which indicated the smectite gradually dominated in the nanocomposite. Because the interlayer spaces of smectite provided accessible sites for aflatoxin adsorption, reducing the ratio of PAM in the nanocomposite was expected to offer more available binding sites for aflatoxins to improve the adsorption capacity of smectite-PAM nanocomposite films. If the PAM concentration was too low (e.g., <0.001%), however, there would not be enough polymer for binding the negatively-charged smectite, thereby resulting in non-uniform assembly and poor structural stability of the nanocomposite in liquid solutions. Therefore, a proper PAM/smectite ratio proved to be critical for achieving high film quality and stability while maintaining good adsorption capacity. Based on the uniformity of the nanocomposite films and the XRD results, the optimal PAM concentration was determined to be 0.005% under the current assembly conditions. The

scanning electron micrographs (SEM) (Figure 10) of the smectite-PAM nanocomposite films assembled from 0.005% PAM solutions suggested a relative uniform coating of the nanocomposite on the silicon wafer.

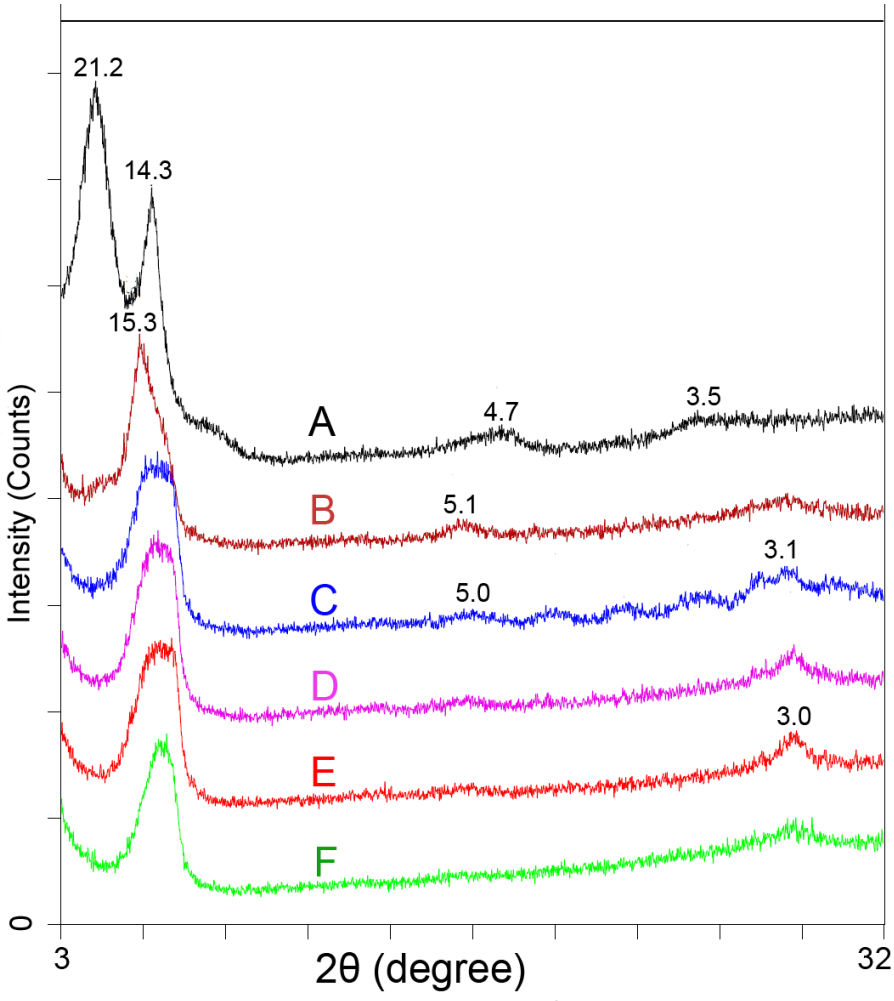

Figure 9. XRD patterns of the smectite-PAM nanocomposite films assembled from PAM solutions with different concentrations: (A) 0.8%, (B) 0.1%, (C) 0.05%, (D) 0.01%, (E) 0.005%, and (F) 0.001%.

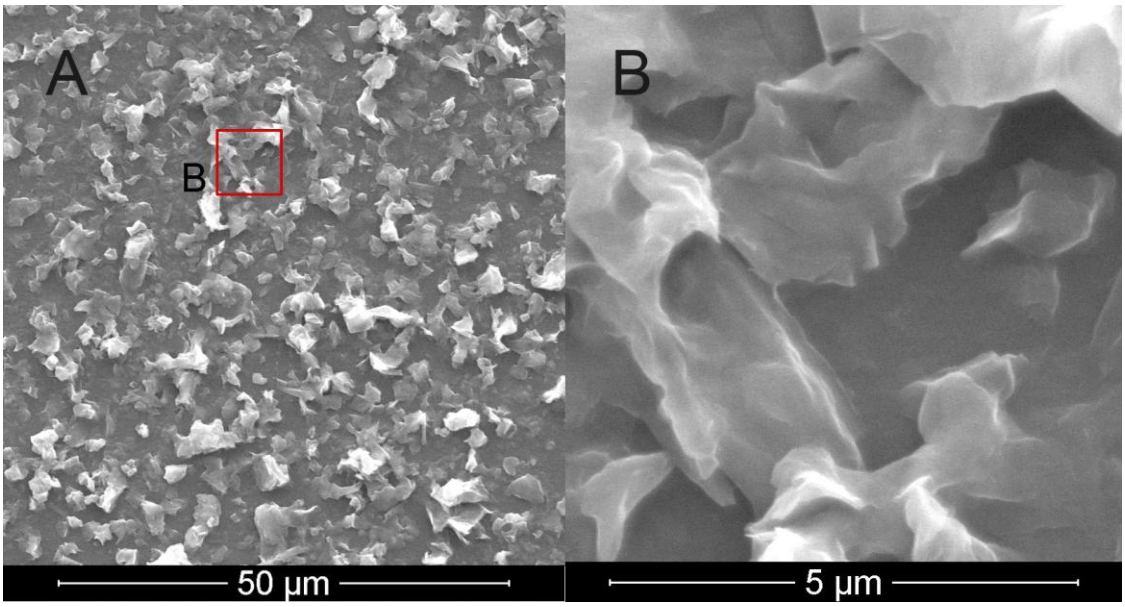

Figure 10. SEM images of surfaces of the smectite-PAM nanocomposite film assembled from 0.005% PAM solution under different magnifications: (A) 1000 × and (B) 10000 ×.

3.3.2 Fluorescence spectra from adsorbed aflatoxins on smectite-PAM nanocomposite films

On the fluorescence spectra (Figure 11a and 11c) of AFB_1- and AFG_1-adsorbed smectite-PAM nanocomposite films, the peak fluorescence intensity (Figure 11e) increased nearly linearly with the original concentration of aflatoxins up to 100ppb. For AFB_2 and AFG_2 (Figure 11b and 11d), the peak fluorescence intensity started to saturate if the aflatoxin concentration was higher than certain values (Figure 11f). Since the peak fluorescence intensity was nearly proportional to the concentration of the adsorbed aflatoxin [6], this phenomenon indicated that the nanocomposite film had a lower adsorption capacity of AFB_2 and AFG_2. Further studies on the molecular smectite-

aflatoxin binding mechanisms will be conducted to investigate the difference in the adsorption affinity of different types of aflatoxins even though they have similar molecular structures.

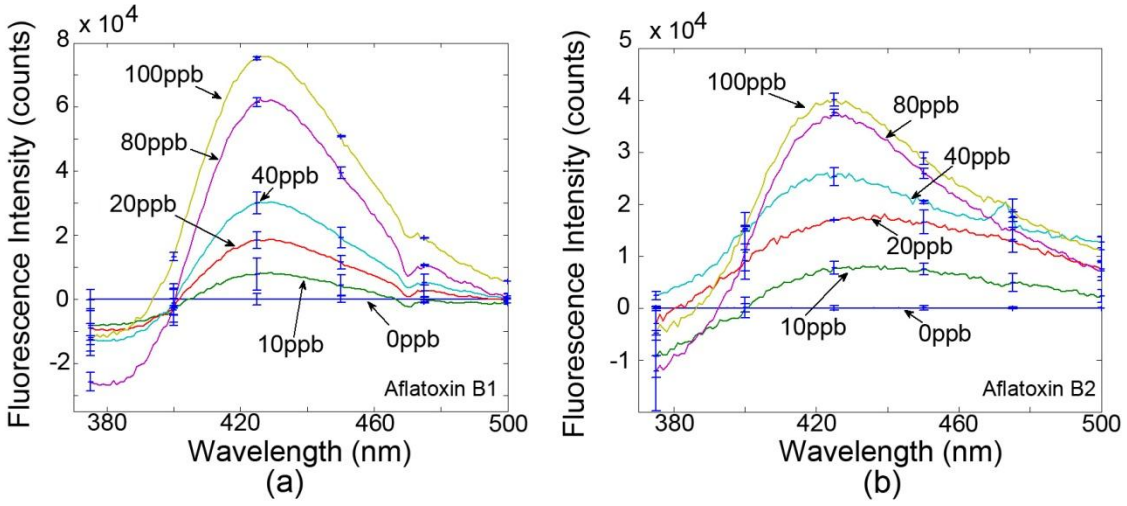

Figure 11. (a)(b) Fluorescence spectra of AFB_1- and AFB_2- adsorbed smectite-PAM nanocomposite films; (c)(d) Fluorescence spectra of AFG_1- and AFG_2- adsorbed smectite-PAM nanocomposite films; (e) Fluorescence intensities (at 432nm) of AFB_1- and AFB_2- adsorbed smectite-PAM nanocomposite films vs. original aflatoxin concentrations in the test solutions; (f) Fluorescence intensity (at 452nm) of AFG_1- and AFG_2- adsorbed smectite-PAM nanocomposite films vs. original aflatoxin concentration in the test solutions.

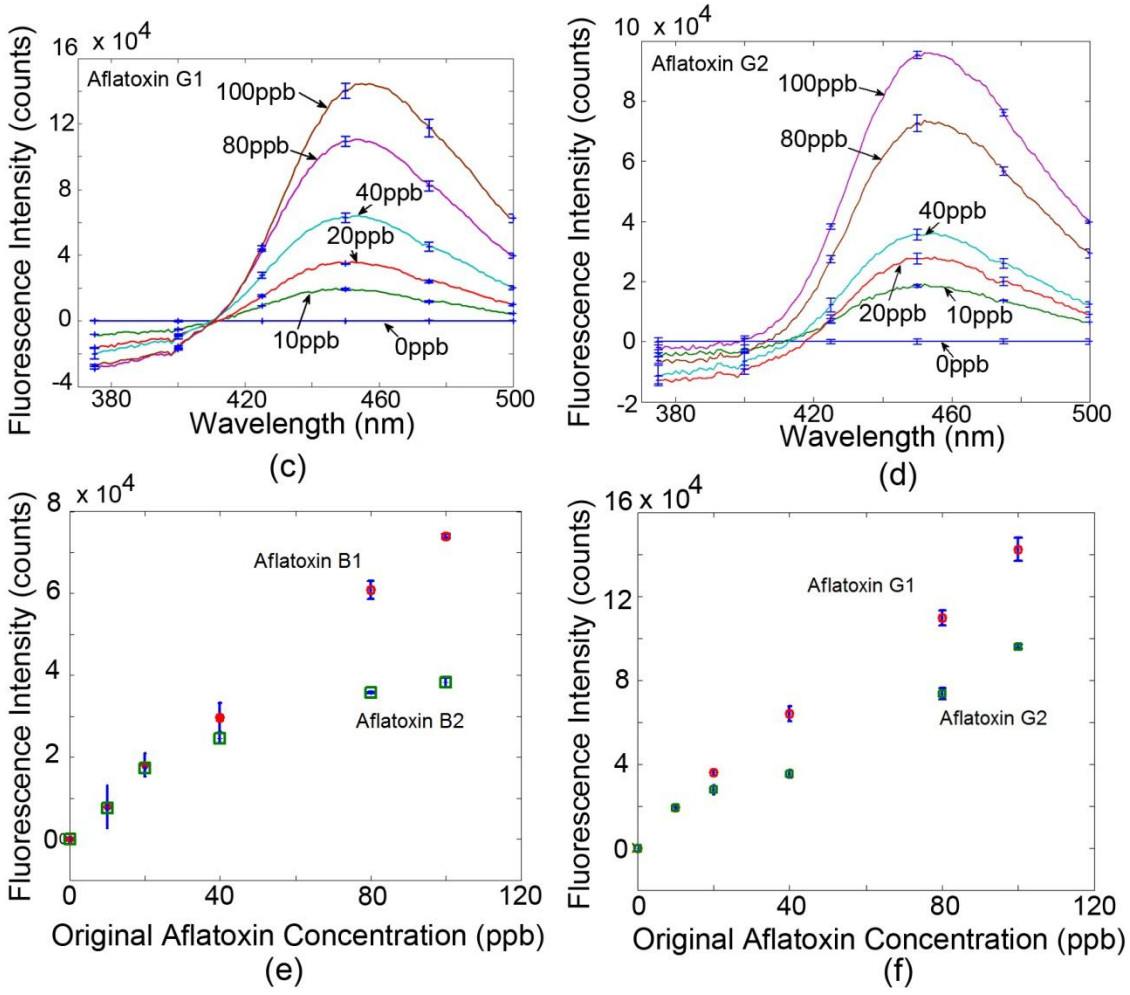

Figure 11. Continued

3.3.3 Fluorescence spectra from aflatoxin mixtures adsorbed on the smectite-PAM nanocomposite films

For the tests on AFB_1/AFB_2 and AFG_1/AFG_2 mixtures, below 50 ppb, the peak fluorescence intensity of aflatoxin-adsorbed nanocomposite films increased linearly with the total aflatoxin concentration in the solution (Figure 12). Based on the peak fluorescence intensity values from 20 blank samples immersed in DI water, the limit of detection (LOD) was 3.60 ppb (estimated by average blank value plus 2 times standard deviation of the blank) for AFB_1/AFB_2 mixture and 1.82 ppb for AFG_1/AFG_2 mixture; the limit of quantification (LOQ) was 17.99 ppb (estimated by average blank value plus 10 times standard deviation of the blank) for AFB_1/AFB_2 mixture and 10.35 ppb for AFG_1/AFG_2 mixture [22].

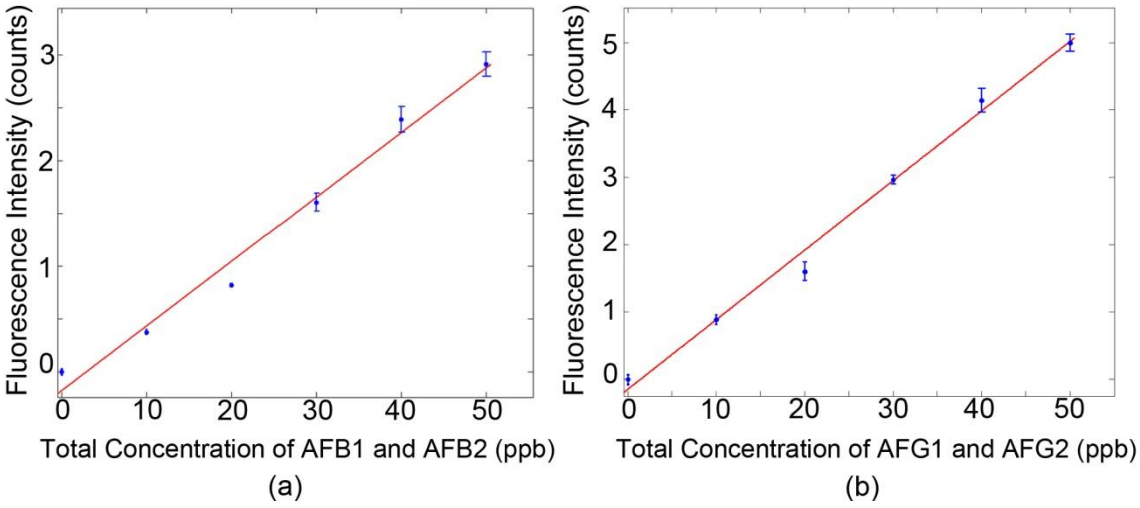

Figure 12. (a)Fluorescence intensity at 432nm vs. total concentration of the AFB_1/AFB_2 mixture in the corn extraction solutions; (b)Fluorescence intensity at 452nm vs. total concentration of the AFG_1/AFG_2 mixture in the corn extraction solutions.

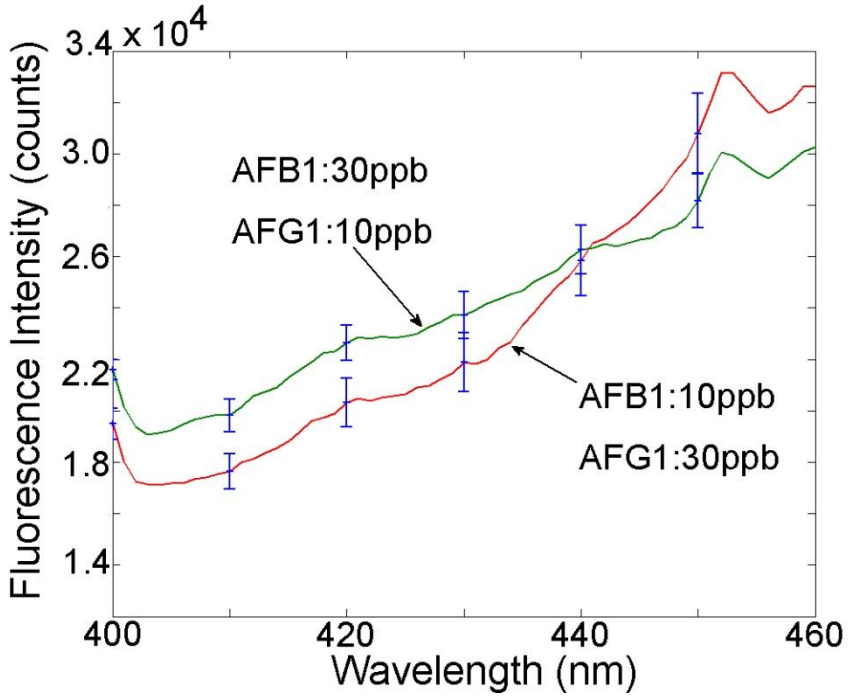

Figure 13. Fluorescence spectra of AFB_1 and AFG_1 adsorbed smectite-PAM nanocomposite films.

Fluorescence spectra of AFB_1/AFG_1-adsorbed smectite-PAM nanocomposite films were recorded (Figure 13). No visible fluorescence peaks were observed, which was due to the overlap of the fluorescence peaks of AFB_1 (around 432 nm) and AFG_1 (around 452 nm). Therefore, fluorescence intensities at 432 nm (for AFB_1) and 452 nm (for AFG_2) were recorded. Table 1 lists the average fluorescence intensities (at 432 nm and 452 nm) from two groups of AFB_1/AFG_1-adsorbed smectite-PAM nanocomposite films. The AFB_1/AFG_1 concentrations were 10/30 ppb and 30/10 ppb, respectively. At this low level of concentration, the peak fluorescence intensity from the aflatoxin adsorbed smectite-PAM films was proportional to the original concentration of the

aflatoxin spiked corn extraction solutions. Based on this linear relationship, the following relations can be derived:

$$K_{11}C_1 + K_{12}C_2 = I_1 \tag{3.1}$$

$$K_{21}C_1 + K_{22}C_2 = I_2 \tag{3.2}$$

where I_1 and I_2 (unit: counts) are the fluorescence intensities at 432 nm and 452 nm, C_1 and C_2(unit: ppb) are the original concentrations of AFB_1 and AFG_1, respectively, and K_{11}~K_{22}(unit: counts/ppb) are their correlation coefficients, the values of which are listed as follows.

$$K_{11} = 6.32 \times 10^2, K_{12} = 5.23 \times 10^2 \tag{3.3}$$

$$K_{21} = 7.13 \times 10^2, K_{22} = 8.68 \times 10^2 \tag{3.4}$$

Table 1. Fluorescence intensities of smectite-PAM nanocomposite films tested in two groups of AFB_1/AFG_1spiked corn extraction solutions.

Sample Number	Concentration of Aflatoxins (ppb)		Fluorescence Intensity ($\times 10^4$counts)	
	B_1	G_1	At 432 nm	At 452 nm
1	10	30	2.2002	3.3168
2	30	10	2.4184	3.0074

In order to test the accuracy of the estimated correlation coefficients (K_{11}~K_{22}), another two groups of AFB_1/AFG_1 spiked corn extract solutions were also prepared. The original AFB_1/AFG_1 concentrations in these three groups of solutions are 10/10 ppb and 20/20 ppb, respectively. AFB_1/AFG_1 adsorption experiments were

conducted and the fluorescence spectra from the AFB_1/AFG_1 adsorbed smectite-PAM nanocomposite films were characterized (Figure 14). Based on the fluorescence intensity at 432 nm and 452 nm and the previously estimated values of the correlation coefficients (K_{11}~K_{22}), the original AFB_1/AFG_1 concentration in the test solution was predicted and the recovery rate and coefficient of variation (CV) were also calculated (Table 2). As listed in Table 2, when the total aflatoxin concentration was less than 40 ppb, the recovery ranged from 90.52% to 110.11%, and the coefficient of variation (CV) was less than 8%.

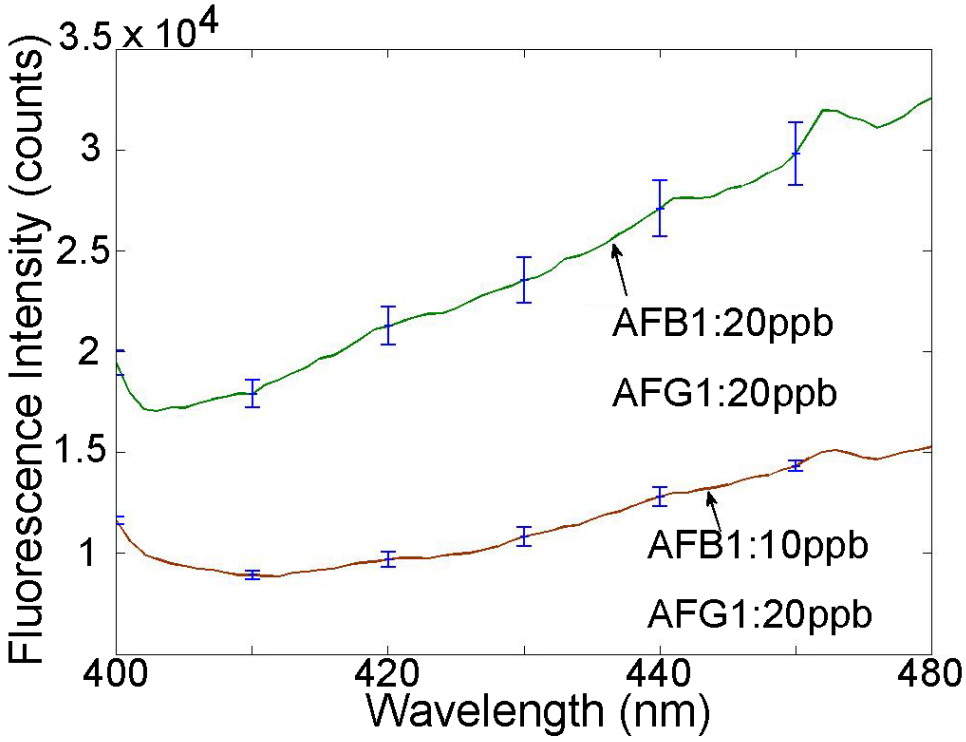

Figure 14. Fluorescence spectra of AFB_1 and AFG_1 adsorbed smectite-PAM nanocomposite films.

Table 2. Recovery rates of aflatoxin B_1 and G_1 from corn extraction solutions.

Sample Number	Concentration of Aflatoxins (ppb)		Mean±SD (ppb)		Recovery (%)		CV (%)	
	B_1	G_1	B_1	G_1	B_1	G_1	B_1	G_1
1	10	10	9.32±0.52	9.99±0.26	93.19±7.15	99.91±3.55	5.58	2.60
2	20	20	22.02±1.62	18.10±1.40	110.11±9.79	90.52±7.43	7.36	7.73

3.4 CONCLUSIONS

In this study, we have successfully demonstrated the optimization of layer-by-layer assembled smectite-PAM nanocomposite films as the molecular capturing agents for the quantification of different types of aflatoxins at sub-100 ppb levels. The cation exchange of Ca^{2+} with Ba^{2+} and the fine-tuning of the polymer loading were shown to be effective to improve the adsorption property of in the smectite-PAM nanocomposite film, while maintaining its structural stability. This improved adsorption property made it possible to capture and concentrate the aflatoxin molecules even at ppb levels, thereby to enable reliable fluorometric quantification of not only single type, but also different sub-groups of aflatoxins.

4. A MICROFLUIDIC SMECTITE-POLYMER NANOCOMPOSITE(SPN) STRIP SENSOR FOR AFLATOXIN DETECTION

4.1 INTRODUCTION

In the last two sections, a new smectite-polymer nanocomposite thin-film was synthesized and optimized for aflatoxin quantification. By using the smectite-polymer nanocomposite thin film as the capturing agent, the detection of different types of aflatoxin and its mixtures at the concentration as low as 10 ppb has been achieved based on a fluorometric approach. However, the required reaction time was more than 50 min, which was limited by the slow diffusion of aflatoxin molecules in the test solution, especially at extremely low concentrations. In addition, to conduct fluorometric measurements, a sophisticated spectrometer was indispensable to characterize the fluorescence emission spectra from the adsorbed aflatoxin molecules, which otherwise would be difficult to operate in the field.

To address the above two issues, a new microfluidic smectite-polymer nanocomposite strip sensor for aflatoxin detection was successfully developed. The use of microfluidic channels to confine the flow of the aflatoxin solution to a close proximity of the smectite-polymer nanocomposite surface, thereby significantly shortening the diffusion length and time of the aflatoxin molecules prior to their adsorption. As a result, the total detection time has been reduced to 10~20 min. In addition, by leveraging the fluorescence excitation modulation, quantitative detection of aflatoxin concentration (5~100 ppb) in the corn extraction has been successfully achieved without the use of a

spectrofluorometer.

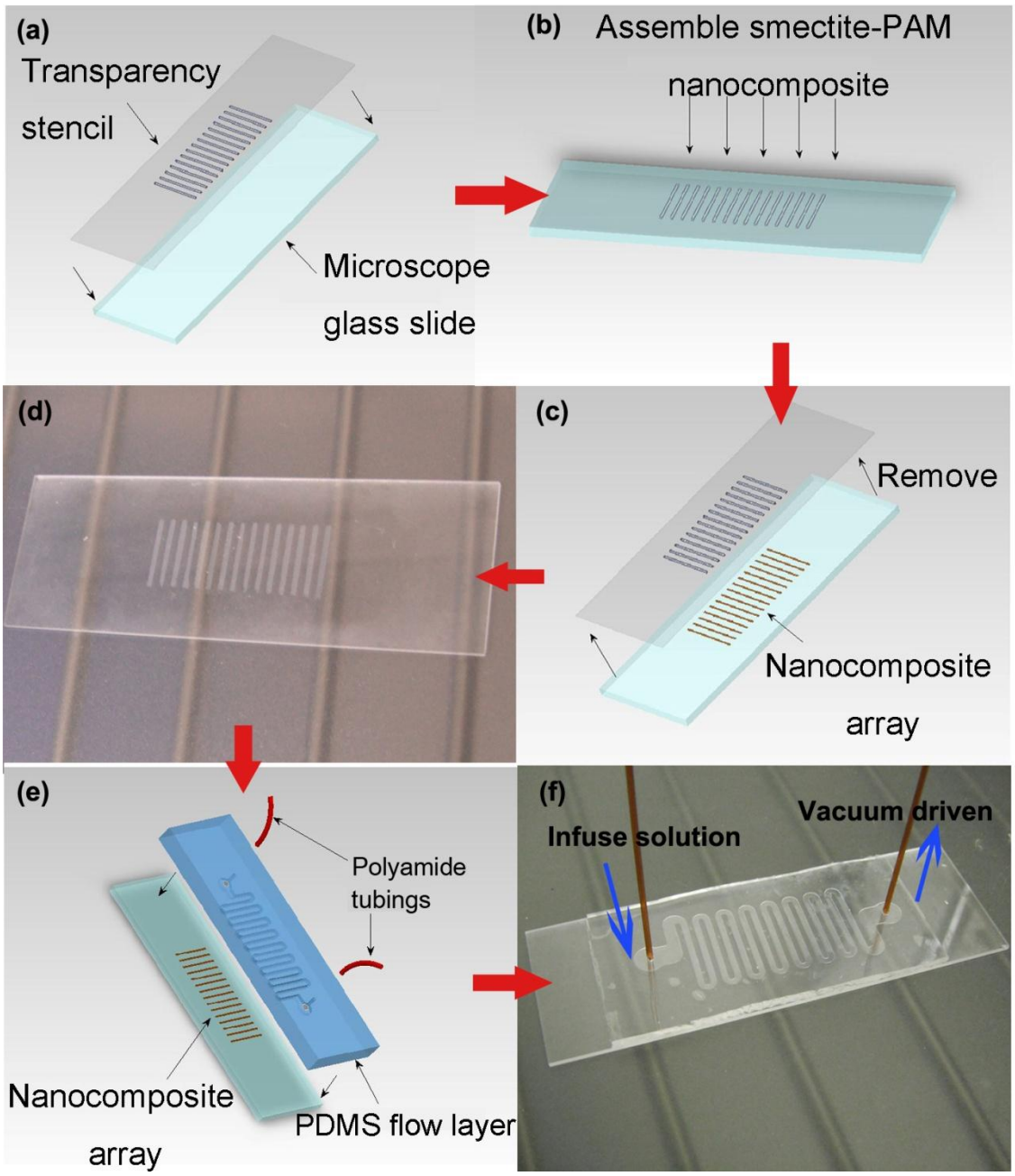

Figure 15. Microfluidic chip fabrication process: (a) Transparency stencil was attached to a microscope glass slide; (b) Smectite-PAM nanocomposite was assembled onto the surface of the glass slide; (c) Transparency stencil was removed; (d) Smectite-PAM nanocomposite strips were formed on the glass slides; (e) PDMS flow layer was attached to the surface of the glass slide; (f) A completed microfluidic sensor device.

4.2 SENSOR FABRICATION

The Greek calcium bentonite obtained from the S&B Industrial Minerals S.A. (1934-now, Athens, Greece) was used in this research. Smectite suspension was prepared following the procedures in last sections. In order to improve the aflatoxin adsorption capacity of the smectite, Ca^{2+} in the original smectite was exchanged with Ba^{2+} by following the modification procedures in the last section. Smectite-polyacrylamide (PAM) nanocomposite strips were formed on a glass slide through the layer-by-layer assembly process. Microscope glass slides (75mm×25mm×1mm) were used as the substrates to make the smectite-PAM nanocomposite strips. A stencil (Figure 15a) was trimmed out of a printing transparency sheet by using a laser cutting machine (Professional series, Universal Laser System Inc.). On the stencil, 15 regularly spaced rectangular openings (10mm×0.5mm each) were used to define the smectite-PAM nanocomposite strips on the glass substrate. Before the layer-by-layer assembly process (Figure 15b), the stencil was attached to the glass slide, and they were clamped together by two 0.75" wide binder clips (Officemate International Corporation, Edison, NJ, USA). After layer-by-layer assembly process, the stencil was removed (Figure 15c), which left the well-defined smectite-PAM nanocomposite strips on the glass substrate (Figure 15d).

The fabrication of the microfluidic chip followed the standard microfluidic device protocol [26]. First the pattern of the designed flow layer was translated into a positive structure on a silicon wafer (3" Test wafers, University Wafer, Inc. South Boston, MA) using SU-8 100 negative photoresist (MicroChem, Newton, MA). A

photolithography process was adapted based on the manufacturer suggested recipe [27]. After being cleaned with isopropyl alchohol and deionized water, it was used as a mould to form ~5 mm thick polydimethylsiloxane (PDMS, *Sylgard 184*, Dow Corning) flow layer of the microfluidic chip. The height of the flow channel was about 100μm. Holes serving as access ports to the flow channel were punched out. Both the glass slide with the nanocomposite strips (obtained from the last step) and the PDMS replica were treated with O_2 plasma for 30 s to activate the surfaces. Then they were brought into contact immediately to enclose the smectite-PAM nanocomposite strips in the flow channel (Figure 15e). Two polymide tubings (#285, diameter 0.72mm, MicroLumen Inc. FL) were connected to the access holes and sealed with RTV 108 Translucent Adhesive (Momentive Performance Materials Inc., OH) (Figure 15f).

4.3 TEST AND CHARACTERIZATION

4.3.1 Test procedures

AFB_1-spiked corn extraction solution was prepared following the standard aflatoxin extraction and analysis procedures used in the previous section. AFB_1 was spiked into corn extracts to achieve the following concentrations: 0, 5, 10, 15, 20, 40, 60 and 80 ppb. For each of the solutions containing 5, 10 and 15 ppb aflatoxins, 20 mL test solution was passed through one flow channel twice and the whole flowing process last around 20 min. For the solutions with higher aflatoxin concentrations, only half of the volume (10 mL) of test solution was passed through the channels, which decreased the flowing time to about 10 min.

The above test steps were repeated for all the corn extracts in each group. After this step, the PDMS layer was peeled off to expose the AFB_1-adsorbed smectite-PAM nanocomposite strips. The fluorescence emission from the nanocomposite strips under both normal and oblique UV illumination (365nm) was recorded using a regular photo camera (Canon PowerShot S95).

4.3.2 Test results

Photos of AFB_1-adsorbed smectite-PAM nanocomposite strips under the normal/oblique UV illumination were taken (Figure 16a and 16b). The fluorescence emission from the smectite-PAM nanocomposite strips on the same glass slide was uniform under normal illumination. But under oblique illumination, as the distance between a nanocomposite strip and the UV lamp increased, the fluorescence intensity from the strip decreased gradually. The phenomenon can be explained as follows. According to a three-level radiative quantum system model [28] for a fluorescence molecule, the rate R at which a fluorescence dipole emits photons is given by

$$R(I) = R_\infty \frac{I / I_s}{1 + I / I_s} \tag{4.1}$$

where I is the intensity of the exciting light and R_∞ and , I_s are two constants determined by the type of the fluorescence molecule. R_∞ and I_s describe the saturation behavior of the emission rate. Since the excited state has a finite lifetime, the average time between two emission photons is limited to a finite value. The typical value of I_s is 3 kW/cm^2 at 500 nm [28]. For the weak excitation ($I/I_s \ll 1$), R is approximately proportional to the excitation intensity I. In our testing setup, the total power of the UV lamp is 3 W and

area of the window of the lamp is 3.5cm×4.5cm. Therefore, the maximum intensity I of the illumination UV light is less than 0.19 W/cm^2, much smaller than I_s. Therefore, the fluorescence molecules (AFB_1) under the oblique UV incidence should be in the weak excitation mode. The average radiative decay rate $\langle R \rangle$ of fluorescence molecules was approximately proportional to the excitation intensity I,

$$\langle R \rangle \propto I \tag{4.2}$$

Their total fluorescence intensity I_{fi} was proportional to the product of the AFB_1 concentration C_i and their average radiative decay rate $\langle R \rangle$,

$$I_{fi} \propto C_i \langle R \rangle \tag{4.3}$$

Therefore,

$$I_{fi} \propto C_i I \tag{4.4}$$

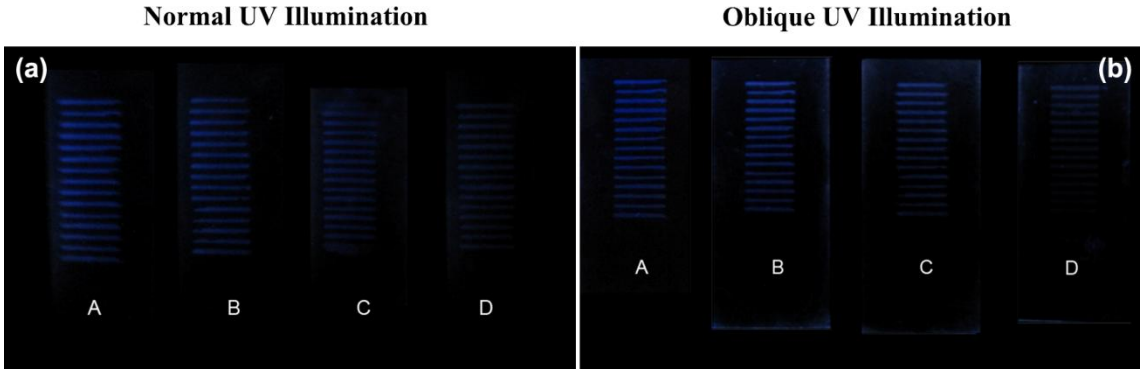

Figure 16. (a) AFB1 adsorbed nanocomposite strips under normal UV incidence (A, B, C and D are slides); (b) AFB1 adsorbed nanocomposite strips under oblique UV incidence (A, B, C and D are slides); (c) normal illumination setup; (d) oblique illumination setup; (e) fluorescence intensity distribution on the nanocomposite strips under the normal illumination; (f) fluorescence intensity distribution on the nanocomposite strips under the oblique illumination.

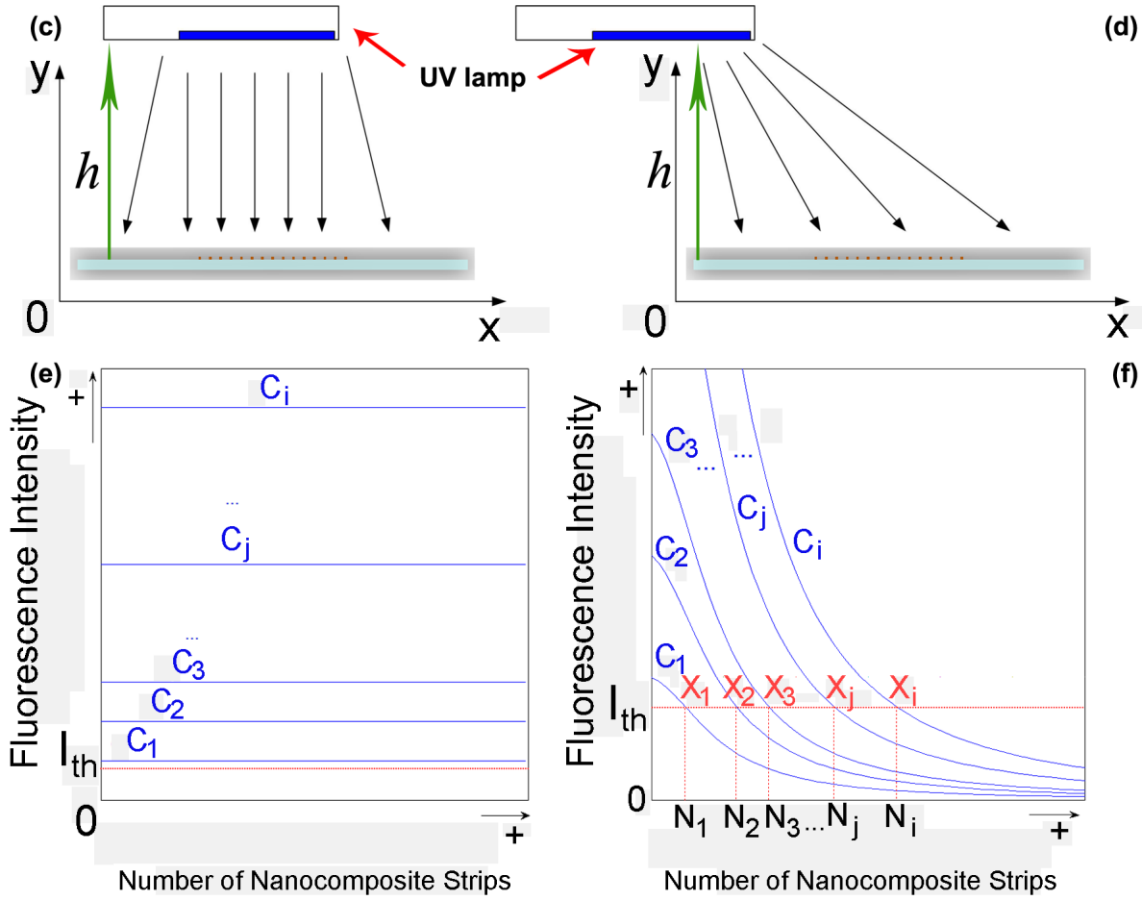

Figure 16. Continued.

As shown in Figure 16c, the normal UV illumination created a uniform illumination field over the entire substrate. According to Eq. 4.4, the uniform fluorescence emission (I_{fi}) from the aflatoxin-adsorbed nanocomposite strips (Figure 16e) indicated a uniform aflatoxin adsorption, which could be explained by the relatively fast flow velocity of the test solution in the PDMS microchannel and the relatively slow adsorption process. As a general trend, the intensity of fluorescence emission intensity decreased with the aflatoxin concentration in the test solution. As shown in Figure 16d,

the oblique UV illumination created a non-uniform illumination field with large gradient along the +x direction. As an approximation, a point illumination source model is used to represent the UV lamp. The average excitation intensity $I(x)$ on the nanocomposite strip at the location x is,

$$I(x) = \frac{I_0}{h^2 + x^2} \tag{4.5}$$

Therefore, the fluorescence intensity $I_{fi}(x)$ of this nanocompsite strip is,

$$I_{fi}(x) \propto C_i \frac{I_0}{h^2 + x^2} \tag{4.6}$$

Figure 16f shows a group of $I_{fi}(x)$ curves for different AFB_1 concentrations (C_i). A threshold fluorescence intensity I_{th} exists, which represents weakest fluorescence that can be visually distinguished. The intercept point between the $I_{fi}(x)$ curves and the I_{th} line determines the number of nanocomposite strips (N_j), which can be effectively observed visually. Higher AFB_1 concentration in the test solution leads to more adsorption on the nanocomposite strips and larger number of observable nanocomposite strips. This correlation makes it possible to achieve a quantitative estimation of AFB_1 concentration in the test solution by just counting the number of "fluorescing" nanocomposite strips without involving sophisticated spectrofluorometers. Based on this approach, two groups of AFB_1-spiked corn extraction solutions were quantified (Figure 17). At the low concentration level (5 ppb, 10 ppb and 15 ppb), an accuracy of $\pm$5ppb was achieved by flowing 20 mL of test solution. For the high concentration group, an accuracy of $\pm$10 ppb was achieved by flowing 10 mL of test solution.

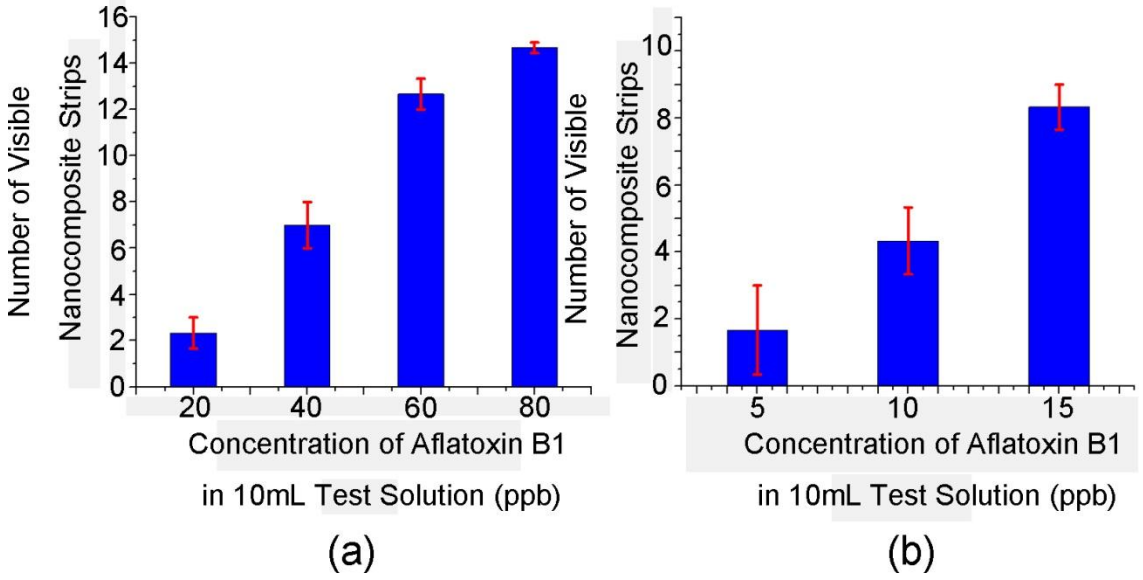

Figure 17. The testing results on two concentration levels: (a) from 20 ppb to 80ppb, 10mL; (b) from 5 ppb to 15 ppb, 20mL.

4.4 CONCLUSION

In this section, a smectite-PAM nanocomposite based strip sensor for rapid quantification of aflatoxins in corn extraction solutions was developed. Microfluidic channels were used to reduce the diffusion length and time of aflatoxin adsorption, which resulted in a much shorter detection time. By using incident intensity modulation, a simpler fluorometric quantification of aflatoxin concentration on sub-100 ppb levels was achieved without the need of a dedicated fluorometer. The high sensitivity, fast detection time, simple operation and low cost of the new strip sensor make it especially suitable for field testing applications.

5. SUMMARY AND CONCLUSIONS

A new aflatoxin quantification technology was developed in this study. First, a novel smectite-polymer nanocomposite film for aflatoxin quantification was fabricated through a layer-by-layer assembly method. Several initial tests on its affinity for aflatoxins were conducted. Next, based on the test results, the optimization of the nanocomposite film fabrication procedures was investigated. The optimized smectite-polymer nanocomposite was able to quantify aflatoxins in food extraction solutions at ppb-level concentrations. Finally, a microfluidic aflatoxin quantification chip based on smectite-polymer nanocomposite films was designed and tested.

In the fabrication of the smectite-PAM nanocomposite film, a layer-by-layer assembly method was taken. Different reaction times were tested, and according to the test results, suitable reaction times for each step in the layer-by-layer assembly process were fixed. Surface morphology and cross-section of the nanocomposite film were recorded by a SEM system. In the aflatoxin adsorption and quantification tests, a group of 2 mL corn extraction solutions containing different amounts of AFB_1 were tested by smectite-PAM nanocomposite films. According to the test results, it could be concluded that when the AFB_1 concentration was lower than 1 ppm in 2 mL corn extraction solution, the AFB_1 molecules adsorbed by the nanocomposite film were proportional to the concentration. Above 1 ppm, the nanocomposite film would be saturated by the aflatoxins. From 50 ppb to 1 ppm, AFB_1 in the corn extraction solutions could be linearly quantified by measuring the fluorescence intensity from the nanocomposite

films. In the additional tests, two groups of smectite-PAM nanocomposite films were immersed into AFB_1 test solutions. One group were agitated by orbital shaker during the immersion step, but the other group were not. The test results demonstrated that the competing molecules from the corn extraction solution would not interfere with the AFB_1 adsorption. And the agitation could increase the diffusion and adsorption of AFB_1.

The smectite-PAM nanocomposite film was optimized so as to improve its aflatoxin adsorption capacity. In order to enhance the size matching between interlayer adsorbing sites in the smectite and afltoxin molecules, the cations (e.g., Ca^{2+}) were exchanged with those with a larger radius (Ba^{2+}). Polymer ratio in the nanocomposite was another factor that would affect the aflatoxin adsorption. Tests were conducted to find an optimized smectite-polymer ratio. The results showed that smectite-PAM nanocomposite films made from 0.005% PAM solutions had a relative uniform surface and a low polymer ratio. With the optimized nanocomposite films, aflatoxins in the food extraction solutions at a low concentration (below 20ppb) were able to be quantified. The selectivity of the nanocomposite film on different types of aflatoxins (AFB_2, AFG_1 and AFG_2) was investigated. A new multi-type aflatoxins fluorometric quantification method was developed, and its accuracy was verified.

Through the above work, a smectite-polymer nanocomposite for aflatoxin quantification has been developed. But the detection and quantification process was still limited to the lab. So a portable device for the aflatoxin quantification was designed and made. This microfluidic detection chip was made following a typical microfluidic channel fabricated process. The nanocomposite strips were deposited into the channels.

The microfluidics technology helped reduce the time of the whole quantification process. A quantification method based on a lab use UV lamp was developed. The UV lamp replaced the spectrofluorometer which was expensive and time-consuming for the aflatoxin quantification. The nanocomposite film and the aflatoxin detection chip developed in this study are hopeful to offer a new way for aflatoxin detection and quantification in food and feed industry.

REFERENCES

[1] G. S. Shephard, Mycotoxins in the context of food risks and nutrition issues, in: D. Barug, The mycotoxin factbook: food & feed topics, Wageningen Academic Pub, 2006, pp. 21-36.

[2] M. V. Trucksess, A. E. Poland, Mycotoxin Protocols: Methods in Molecular Biology, vol. 157, Human Press, Totowa, New Jersey, 2001.

[3] J. Gilbert, E. A. Vargas, Advances in sampling and analysis for aflatoxins in food and animal feed, J. Toxicol. 22 (2003) 381-422.

[4] B. S. Delmulle, S. M. D. G. D. Saeger, L. Sibanda, I. B. Vetro, C. H. V. Peteghem, Development of an immunoaasay-based lateral flow dipstick for the rapid detection of aflatoxin B_1 in pig feed, J. Agric. Food Chem. 53 (2005) 3364-3368.

[5] K. E. Sapsford, C. R. Taitt, S. Fertig, M. H. Moore, M. E. Lassman, C. M. Maragos, L. C. Shriver-Lake, Indirect competitive immunoassay for detection of aflatoxin B_1 in corn and nut products using the array biosensor, Biosens. Bioelectron. 21 (2006) 2298-2305.

[6] J. A. A. Ho, R.D. Wauchope, A strip liposome immunoassay for aflatoxin B_1, Anal. Chem. 74 (2002) 1493-1496.

[7] X. Sun, X. Zhao, J. Tang, J. Zhou, F. S. Chu, Preparation of gold-labeled antibody probe and its use in immunochromatography assay for detection of aflatoxin B_1, Int. J. Food Microbiol. 99 (2005) 185-194.

[8] A. Y. Kolosova, W. Shim, Z. Yang, S. A. Eremin, D. Chung, Direct competitive ELISA based on a monoclonal antibody for detection of aflatoxin B_1. Stabilization of ELISA kit components and application to grain samples, Anal. Bioanal. Chem. 384 (2006) 286-294.

[9] T. N. Pasha, M. U. Farooq, F. M. Khattak, M. A. Jabbar, A. D. Khan, Effectiveness of sodium bentonite and two commercial products as aflatoxin absorbents in diets for broiler chickens, Anim. Feed Sci. Technol. 132 (2007) 103-110.

[10] Y. Deng, A. L. B. Velázquez, F. Billes, J. B. Dixon, Bonding mechanisms between aflatoxin B_1 and smectite, Appl. Clay Sci. 50 (2010) 92-98.

[11] I. Kannewischer, M. G. T. Arvide, G. N. White, J. B. Dixon, Smectite Clays as Adsorbents of Aflatoxin B_1: Initial Steps, Clay Sci. 12 (2006) 199-204.

[12] M. Z. Zheng, J. L. Richard, J. Binder, A review of rapid methods for the analysis of mycotoxins, Mycopathologia. 161 (2006) 261-273.

[13] K. Reif, W. Metzger, Determination of aflatoxins in medicinal herbs and plant extracts, J. Chromatogr. A. 692 (1995) 131-136.

[14] C. M. Franco, C. A. Fente, B. Vazquez, A. Cepeda, L. Lallaoui, P. Prognon, G. Mahuzier, Simple and sensitive high-performance liquid chromatography-fluorescence method for the determination of citrinin application to the analysis of fungal cultures and cheese extracts, J. Chromatogr. A. 723 (1996) 69-75.

[15] F. N. Crespilho, V. Zucolotto, O. N. Oliveria Jr., F. C. Nart, Electrochemistry of layer-by-layer film: a review, Int. J. Electrochem, Sci. 1 (2006) 194-214.

[16] Y. Deng, J. B. Dixon, G. N. White, R. H. Loeppert, A. S. R. Juo, Bonding between polyacrylamide and smectite, Colloid Surface A. 281 (2006) 82-91.

[17] Y. Deng, J. B. Dixon, J. N. White, Adsorption of polyacrylamide on smectite, illite and kaolinite, Soil Sci. Soc. Am. J. 70 (2006) 297-304.

[18] J. Jerez, M. Flury, J. Shang, Y. Deng, Coating of silica sand with aluminosilicate clay, J. Colloid Interface Sci. 294 (2006) 155-164.

[19] C. McCormick, Aflatoxin in feeds (corn and cottonseed meal products) by HPLC/PHRED, Protocol No. 16002, Revision No. 004., 2009.

[20] G. E. Morris, M. S. Żbik, Smectite suspension structural behaviour, Int. J. Miner Process. 93 (2009) 20-25.

[21] I. Langmuir, The constitution and fundamental properties of solids and liquids, J. Am. Chem. Soc. 38 (1916) 2221-2295.

[22] D. A. Armbruster, M. D. Tillman, L. M. Hubbs, Limit of detection (LOD)/Limit of Quantitation (LOQ): comparison of the empirical and the statistical methods exemplified with GC-MS assays of abused drugs, Clin. Chem. 40(1994) 1233-1238.

[23] T. D. Phillips, Dietary clay in the chemoprevention of aflatoxin-induced disease, Toxicol. Sci. 52(1999) 118-126.

[24] European Commission. (2001). Regulation (EC). No 466/2001 of 8 March 2001 setting maximum levels for certain contaminants for foodstuffs. Official Journal of European Communities, L77, 1-13.

[25] S. C. Pei, Y. Y. Zhang, S. A. Eremin, W. J. Lee, Detection of aflatoxin M1 in milk products from China by ELISA using monoclonal antibodies, Food Control. 20(2009) 1080-1085.

[26] David C. Duffy, J. Cooper McDonald, Olivier J. A. Schueller, George M. Whitesides, Rapid Prototyping of Microfluidic Systems in Poly(dimethylsiloxane), Anal. Chem. 70(1998) 4974-4984.

[27] Microchem Corp. website, Nano TM SU-8. Available: http://www.microchem.com/products/pdf/SU8_50-100.pdf

[28] L. Novotny, B. Hecht, Principles of Nano-Optics, first ed., Cambridge University Press, Cambridge, 2006.